

# ADVANCES IN A TWO-SOURCE ENERGY BALANCE MODEL: PARTITIONING OF EVAPORATION AND TRANSPIRATION FOR COTTON

P. D. Colaizzi, N. Agam, J. A. Tolk, S. R. Evett,  
T. A. Howell, Sr., S. A. O'Shaughnessy, P. H. Gowda,  
W. P. Kustas, M. C. Anderson



A Tribute to the Career of  
Terry Howell, Sr.

**ABSTRACT.** Accurate partitioning of the evaporation ( $E$ ) and transpiration ( $T$ ) components of evapotranspiration ( $ET$ ) in remote sensing models is important for evaluating strategies aimed at increasing crop water productivity. A two-source energy balance (TSEB) model designed for row crops solves the energy balance of the soil-canopy-atmosphere continuum using surface brightness temperature. By solving the energy balance of the soil and plant canopy separately, the TSEB model can calculate  $E$  and  $T$ , which cannot be done with single-source models. However, few studies have tested the TSEB model where  $E$  or  $T$  measurements were available, which until recently has impeded its advance. This article reviews recent physically based advances of the TSEB model. The advances were tested using measurements of  $E$ ,  $T$ , and  $ET$  by microlysimeters, sap flow gauges, and weighing lysimeters, respectively, at Bushland, Texas, for irrigated cotton having a wide range of canopy cover. Root mean square error (RMSE) and mean bias error (MBE) were  $0.54$  and  $-0.19$   $\text{mm d}^{-1}$ , respectively, between measured and calculated  $E$ . RMSE and MBE were  $0.87$  and  $0.31$   $\text{mm d}^{-1}$ , respectively, between measured and calculated  $T$ . This was deemed an improvement over previous TSEB model versions, which overestimated  $E$  and underestimated  $T$ , resulting in RMSE and MBE of up to  $3.8$  and  $-3.5$   $\text{mm d}^{-1}$ , respectively. Ongoing research includes testing the TSEB model using different remote sensing platforms, from ground-based to satellite scales.

**Keywords.** Evapotranspiration, Irrigation, Remote sensing, Texas.

Evaporation ( $E$ ) and transpiration ( $T$ ) are important pathways of water flux away from irrigated crop surfaces. In cropping systems, biomass production and economic yield are closely related to  $T$  from the plant canopy, whereas  $E$  flux is from the soil beneath the crop or from the canopy surface following rain or irrigation, which do not directly contribute to yield production. Therefore, increases in crop water productivity usually

seek to minimize  $E$  relative to  $ET$ , so that the  $T/ET$  ratio is maximized (Doorenbos and Kassam, 1979). Because  $E$  and  $T$  are difficult to measure separately, they are often composited as evapotranspiration ( $ET$ ). The relative contributions of  $E$  and  $T$  to  $ET$  are nonetheless important to understanding water flux processes of vegetation, particularly crops, where water is a primary constraint to production (Newman et al., 2006; Kool et al., 2014a; Schlesinger and Jasechko, 2014). As freshwater resources continue to become relatively scarce for agricultural production, along with the uncertainty imposed by climate change, there is increasing interest in  $E$  and  $T$  partitioning in order to find ways to enhance crop water productivity. Consequently, numerous crop, energy balance, and mass balance models of varying complexity have been developed that address this objective (Evet and Tol, 2009). Of these, energy balance approaches designed to use remote sensing (RS) data in reflectance and thermal bands have received significant attention because RS can capture the spatial variation of vegetation characteristics more efficiently than approaches limited to micrometeorological or *in situ* measurements alone, and RS approaches are relatively practical to implement (Gowda et al., 2008; Kustas and Anderson, 2009; French et al., 2015).

One thermal-based energy balance RS approach that calculates  $E$  and  $T$  explicitly is a two-source energy balance model that was initially developed by Norman et al. (1995)

---

Submitted for review in February 2015 as manuscript number NRES 11215; approved for publication by the Natural Resources & Environmental Systems Community of ASABE in July 2015.

Mention of company or trade names is for description only and does not imply endorsement by the USDA. The USDA is an equal opportunity provider and employer.

The authors are **Paul D. Colaizzi**, ASABE Member, Research Agricultural Engineer, USDA-ARS Conservation and Production Research Laboratory (CPRL), Bushland, Texas; **Nurit Agam**, Professor, Blaustein Institutes for Desert Research, Ben-Gurion University of the Negev, Sede-Boqer, Israel; **Judy A. Tol**, Research Plant Physiologist, **Steven R. Evett**, ASABE Member, Research Soil Scientist, **Terry A. Howell Sr.**, ASABE Fellow, Research Agricultural Engineer (retired), **Susan A. O'Shaughnessy**, ASABE Member, Research Agricultural Engineer, and **Prasanna H. Gowda**, ASABE Member, Research Agricultural Engineer, USDA-ARS CPRL, Bushland, Texas; **William P. Kustas**, Hydrologist, and **Martha C. Anderson**, Research Physical Scientist, USDA-ARS Hydrology and Remote Sensing Laboratory, Beltsville, Maryland. **Corresponding author:** Paul D. Colaizzi, USDA-ARS, P.O. Drawer 10, Bushland, Texas, 79012-0010; phone: 806-356-5763; e-mail: paul.colazizzi@ars.usda.gov.

and Kustas and Norman (1999), herein termed the TSEB model. Their TSEB model combines the biophysical characteristics of vegetation with the energy balance of the canopy and soil, but it does not require much greater information compared with thermal-based single-source models, and it requires less information compared with other thermal-based two-source modeling approaches (Kustas and Anderson, 2009). The somewhat greater complexity of the TSEB model has nonetheless been a deterrent to its more widespread use, and the paucity of E and/or T measurements has limited most TSEB model studies to consider only latent heat flux ( $LE$ ) or ET. Among other factors, issues include sensitivity to land surface temperatures, spatial variability of air temperature, the surface-air temperature gradient, and spatial and temporal variability of leaf area index (French et al., 2015). The accuracy of RS-based energy balance models in general is contingent on having available a sufficiently dense network of meteorological stations (Kustas et al., 2012a), along with sufficiently frequent and spatially fine reflectance and thermal measurements (Jackson, 1984). Some approaches, such as those based on time-differencing or sharpening of thermal satellite pixels, have mitigated these issues in the TSEB model with some success (Agam et al., 2007; Anderson et al., 2012; Norman et al., 2000). The recent emergence of wireless mesh networks has made ground-based RS more economical and practical for agricultural applications, and furthermore avoids many pitfalls of airborne and satellite RS (O'Shaughnessy et al., 2013). Moving sprinkler systems, particularly center pivots, can provide a platform to transport radiometers over irrigated fields at regular intervals. Wireless radiometers aboard center pivots can schedule irrigations, resulting in crop water productivity comparable to, or even better than, that achievable using a field-calibrated neutron probe (Peters and Evett, 2008; O'Shaughnessy and Evett, 2010; O'Shaughnessy et al., 2011, 2012). The convergence of commercially available wireless radiometers and increased adoption of center pivots (including on cultivated land not previously irrigated) presents new opportunities to adopt models, such as the TSEB, for routine estimates of E and T using ground-based RS. This could be useful to guide irrigation management and evaluate other crop management strategies aimed at increasing crop water productivity.

Most TSEB model studies have used airborne and satellite imagery (e.g., Anderson et al., 2005; French et al., 2007, 2015; Norman et al., 2000; Li et al., 2005), with fewer studies using ground-based data (e.g., Anderson et al., 2012; Colaizzi et al., 2012a; Kustas et al., 2012a). The partitioning of the vegetation and soil components of ET was somewhat less critical for the larger spatial scale of airborne and satellite pixels compared with the smaller scale of ground-based radiometers, but could not be ignored. This was especially true of row crop vegetation that partially covers the soil, which has a periodic (i.e., non-random) spatial distribution. Therefore, the empirically based clumping index approach developed for forest canopies (Chen and Cihlar, 1995) was adopted for row crops (Anderson et al., 2005). This was effective at partitioning vegetation and soil for pixels, but it proved inadequate for

ground-based radiometers, which usually have elliptical footprints when deployed at oblique viewing angles. Although the oblique angle maximizes the proportion of vegetation appearing in the footprint, soil may still appear in the background, which must be accounted for (Kimes, 1983). Therefore, Colaizzi et al. (2010) developed a geometric view factor procedure for row crops to calculate the proportion of vegetation and soil appearing in the radiometer footprint; these could be further partitioned into their sunlit and shaded components, which was useful for detailed crop biophysical models (e.g., Fitzgerald et al., 2005). The procedure represented crop row vegetation as elliptical hedgerows, which was convenient for projecting the radiometer footprint onto its three-dimensional surface. The procedure was expanded and combined with the Campbell and Norman (1998) radiative transfer model to partition net radiation ( $R_N$ ) to the soil and canopy (Colaizzi et al., 2012b, 2012c). The radiometer footprint and radiation partitioning procedures were applied to the TSEB model and compared with the clumping index approach of Anderson et al. (2005). These were tested against ET measured by large monolithic weighing lysimeters (Marek et al., 1988; Howell et al., 1995) in a highly advective environment for corn, cotton, grain sorghum, and winter wheat (Colaizzi et al., 2012a). Although this study used ground-based IRTs for thermal data, the approach could also be applied to airborne or satellite imagery.

The Bushland Evapotranspiration and Agricultural Remote Sensing Experiment of 2008 (BEAREX08) included measurements of E, T, and ET over irrigated cotton using microlysimeters, sap flow gauges, and weighing lysimeters (Evett et al., 2012a; Kustas et al., 2012b). This resulted in a unique dataset with which E and T partitioning could be investigated, in addition to  $LE$  and/or ET, using *in situ* mass and heat balance methods (Agam et al., 2012a) instead of the more commonly used meteorological flux approaches, which have been subject to uncertainties in energy balance closure and sample area influence (Todd et al., 2000; Twine et al., 2000; Alfieri et al., 2012). The TSEB model requires an initial estimate of canopy latent heat flux and canopy temperature (described in the next section). Briefly, the original Norman et al. (1995) TSEB model version used a form of the Priestley-Taylor equation (Priestley and Taylor, 1972) to derive equations used to solve the energy balance. This resulted in good agreement between daily measured and calculated  $LE$  and ET (Anderson et al., 2012; Kustas et al., 2012a); however, Colaizzi et al. (2014) showed that E and T were over- and underestimated, respectively, by up to 5 mm daily. Therefore, following the Norman et al. (1995) secant approach, Colaizzi et al. (2012d) derived equations based instead on the Penman-Monteith equation (Monteith, 1973) to solve the energy balance, which removed much of the bias between measured and calculated E and T. Colaizzi et al. (2014) further compared and discussed differences between the Priestley-Taylor and Penman-Monteith versions of the TSEB model.

Several additional refinements have been applied to variables and procedures used within the TSEB model, but these have not been previously tested. These are described in the next section. Briefly, they include a new method to

calculate surface soil heat flux ( $G_0$ ) that can distinguish between sunlit and shaded soil (Colaizzi et al., 2016a, 2016b); two modifications to the aerodynamic term, including use of the Richardson number in place of the Monin-Obukhov length for stability correction, and use of a buoyancy-based equation for low wind speeds (Kimball et al., 2015); use of the canopy-air temperature average (instead of air temperature) to calculate the slope of the saturation water vapor-temperature relation (Lascano and van Bavel, 2007); and recalculation of all temperature-dependent terms during each iteration of the secant procedure. These refinements were selected to be applied to the TSEB model because they either improved model convergence, or reduced discrepancies between measured and calculated variables, or a combination of both, in these previous studies.

The objectives of this article are to provide a succinct description of the TSEB model that included advances since BEAREX08 and to compare measured and calculated values of  $R_N$ ,  $G_0$ ,  $LE$ ,  $E$ ,  $T$ , and  $ET$  using these more recent refinements to the TSEB model. It is hoped that the description and results presented herein will motivate greater efforts to measure  $E$  and  $T$ , and also lead to more widespread adoption of the TSEB model (or similar two-source models) to study  $E$  and  $T$  partitioning, with the overarching goal of increasing crop water productivity.

## DESCRIPTION OF THE TSEB MODEL

The energy balance of the substrate-canopy-atmosphere is typically based on equating available energy (commonly described as net radiation and surface soil heat flux) with sensible and latent heat fluxes, where stored energy and photosynthesis are assumed negligible:

$$R_N - G_0 = H + LE \quad (1)$$

where  $R_N$  is net radiation,  $G_0$  is surface soil heat flux,  $H$  is sensible heat flux, and  $LE$  is latent heat flux (all units are  $W m^{-2}$ ). Using this sign convention,  $R_N$  is positive toward, and all other terms are positive away from, the canopy or soil.

The TSEB model partitions each term into its canopy and substrate components, except for  $G_0$ , which only applies to the substrate (fig. 1). In agricultural applications with mostly bare soil, the more general term “substrate” is usually replaced with “soil,” which is the convention used herein. Writing equation 1 separately for the canopy and soil energy balances gives:

$$LE_C = R_{N,C} - H_C \quad (2a)$$

$$LE_S = R_{N,S} - G_0 - H_S \quad (2b)$$

where the subscripts  $C$  and  $S$  refer to the canopy and soil, respectively. As with most energy balance models, the TSEB model calculates the  $LE$  components as residuals of the other terms, and  $H$  components are calculated based on temperature gradients and resistances.

Calculation procedures for  $R_{N,C}$  and  $R_{N,S}$  are given by Colaizzi et al. (2012b, 2012d). Briefly, these procedures use a combination of a radiative transfer model (Campbell and Norman, 1998) to calculate the shortwave radiation balance of the canopy and soil, and geometric models to account for the spatial distribution of row crop vegetation (Colaizzi et al., 2010). In the Campbell and Norman (1998) model, shortwave radiation is partitioned into its photosynthetically active (PAR; 400 to 700 nm) and near-infrared (NIR; 700 to 3000 nm) components, which are further par-

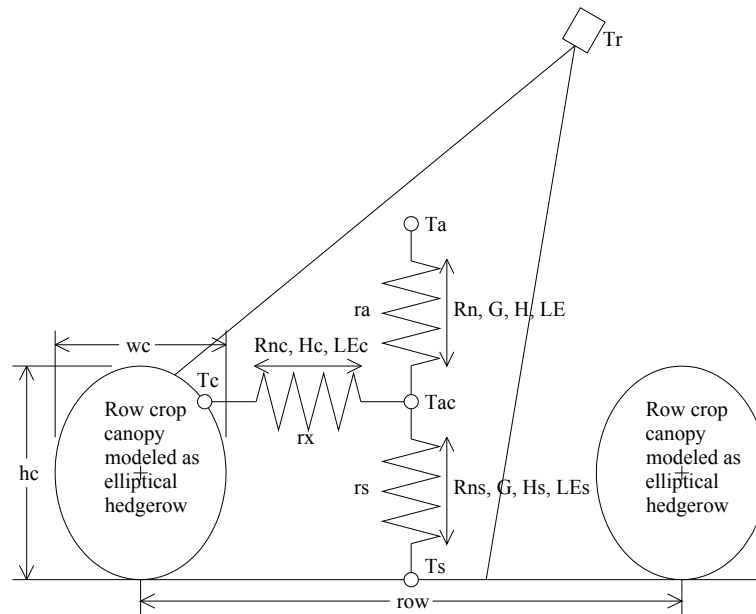


Figure 1. Two-source energy balance (TSEB) model with series resistances for a row crop (based on figure 11 in Norman et al., 1995). A thermal infrared radiometer ( $T_r$ ) aimed obliquely has an elliptical footprint, which can be partitioned between soil and vegetation mathematically given that the vegetation is described as an elliptical hedgerow:  $w_c$  = width of crop row,  $h_c$  = height of crop row,  $T_c$  = temperature of canopy,  $row$  = orthogonal distance between rows,  $T_s$  = soil surface temperature,  $T_{ac}$  = mean of canopy and air temperatures, and  $T_a$  = air temperature. The energy flux terms ( $R_N$ ,  $G$ ,  $H$ , and  $LE$ ) are defined in equations 1, 2a, and 2b.

tioned into their direct beam and diffuse components. This accounts for differences in transmittance, absorption, and reflectance for the canopy and soil for each component. This approach reduced discrepancies between measured  $H$  and  $LE$  and those calculated by the TSEB model (Kustas and Norman, 1999). This approach also reduced discrepancies between measured and calculated transmitted and reflected shortwave radiation over row crops (Colaizzi et al., 2012c) compared with calculating a bulk  $R_N$  and using a simple exponential function (i.e., Beer's law) for component partitioning. Calculation of net longwave radiation to the canopy and soil was based on the Stefan-Boltzmann relation, which required canopy and soil temperatures. Because temperatures and  $R_{N,C}$  and  $R_{N,S}$  also appear in the  $H_C$  and  $H_S$  formulations, an iterative procedure was used. The geometric models were based on representing the canopy as elliptical hedgerows and calculating two view factors for the canopy. The view factors were (1) from the solar zenith angle (i.e., planar view) for shortwave direct beam irradiance and (2) from a downward hemispherical view for shortwave diffuse and longwave radiation (Colaizzi et al., 2012b). Calculation of  $R_{N,C}$  and  $R_{N,S}$  included seven calibrated parameters that were required by the Campbell and Norman (1998) shortwave radiative transfer model, where three were crop specific (i.e., cotton) and four were specific to atmospheric transmittance at the study location (Colaizzi et al., 2012b). The crop-specific parameters included the ellipsoid leaf angle parameter (3.0), PAR leaf absorption (0.83), and NIR leaf absorption (0.14). These values were calibrated using measurements obtained over a different cotton crop (having east-west oriented rows). The atmospheric parameters were weighing factors and exponents for the direct beam portions of PAR (factor = 1.03, exponent = 2.23) and NIR (factor = 1.09, exponent = 2.38) irradiance. These values were calibrated using global and diffuse (i.e., shadow band) irradiance measurements over clipped grass. Three additional parameters were assumed based on previous studies and were not calibrated for this study location. These included soil reflectance for PAR and NIR (0.15 and 0.25, respectively; Campbell and Norman, 1998) and a general canopy longwave extinction coefficient (0.95; Kustas and Norman, 1999).

A new method to calculate  $G_0$  was developed by Colaizzi et al. (2016a). This method was adopted for the present study as:

$$G_0 = \frac{R_{N,S} - R_{N,S,\min}}{R_{N,S,\max} - R_{N,S,\min}} \times (aR_{N,S,\max} - R_{N,S,\min}) + R_{N,S,\min} \quad (3)$$

where  $R_{N,S,\min}$  and  $R_{N,S,\max}$  are the minimum and maximum net soil radiation for a 24 h period ( $W m^{-2}$ ), respectively, and  $a$  is an empirical constant (dimensionless and found to be 0.31 for a clay loam soil at Bushland, Texas, by Colaizzi et al., 2016a, using a different data set). The rationale for this method was to account for sunlit and shaded soil in the crop interrow, which may comprise substantial positional variation of energy balance terms (e.g., Agam et al., 2012b; Kool et al., 2014b). Because calculation of  $R_{N,S}$  includes

view factors, it was straightforward to partition the soil surface into its sunlit and shaded components and calculate sunlit and shaded  $G_0$  accordingly. Although the present study calculated a single  $G_0$  that did not discriminate between sunlit and shaded soil, calculated  $G_0$  better agreed with calorimetrically corrected and calculated  $G_0$  (Colaizzi et al., 2016b) compared with calculating  $G_0$  as a constant (e.g., French et al., 2015) or time-dependent (e.g., Kustas et al., 1998; Santanello and Friedl, 2003) fraction of  $R_{N,S}$ . Furthermore, this method of calculating  $G_0$  required only one additional calibrated parameter ( $a = 0.31$ ) instead of the two or more typically required by other methods. Further refinements to the TSEB model are underway that discriminate between sunlit and shaded surfaces for energy balance terms; these will include calculation of  $G_0$  by equation 3.

The series resistance version of the original TSEB model described by Norman et al. (1995) was used to calculate  $H$ ,  $H_C$ , and  $H_S$  (fig. 1). Series resistances were selected over the alternative parallel resistance formulation to account for turbulent flux exchange between the canopy and soil, which may be significant for partial canopy cover and were found preferable for landscapes having variable canopy cover (Kustas and Norman, 1999; Kustas et al., 2004; Li et al., 2005):

$$H = \rho C_p \frac{T_{AC} - T_A}{r_A} \quad (4a)$$

$$H_C = \rho C_p \frac{T_C - T_{AC}}{r_X} \quad (4b)$$

$$H_S = \rho C_p \frac{T_S - T_{AC}}{r_S} \quad (4c)$$

where  $\rho$  is the density of moist air ( $kg m^{-3}$ ),  $C_p$  is the specific heat of air (assumed constant at  $1013 J kg^{-1} K^{-1}$ ),  $T_C$ ,  $T_A$ ,  $T_S$ , and  $T_{AC}$  are the temperatures of the canopy, air, soil, and air temperature within the canopy boundary layer, respectively (all in K),  $r_A$  is the aerodynamic resistance between the canopy and the air above the canopy ( $s m^{-1}$ ),  $r_X$  is the resistance between the canopy and canopy boundary layer ( $s m^{-1}$ ), and  $r_S$  is the resistance in the boundary layer immediately above the soil surface ( $s m^{-1}$ ). The  $r_A$  term was calculated following Kimball et al. (2015), where stability correction was accounted for through the Richardson number (Mahrt and Ek, 1984) instead of the Monin-Obukhov length (Brutsaert, 1982; Kustas and Norman, 1999). Kimball et al. (2015) reported that using a hybrid Monin-Obukhov length and Richardson number approach resolved convergence problems in their model compared with using the Monin-Obukhov length alone. Although previous TSEB model studies did not have convergence problems using the Monin-Obukhov length (e.g., Colaizzi et al., 2014), the Richardson number formulation was adopted in the present study because it avoided iteration in the  $r_A$  subroutine (hence reducing calculation time) but resulted in little, if any, change to final TSEB model results (data not shown). In the rare case when wind speed was below  $1.0 m s^{-1}$ , we also followed Kimball et al. (2015), where  $r_A$  was calculated following the American Society of Heating, Re-

frigeration, and Air-Conditioning Engineers (ASHRAE) method for an infinite plane having natural convection. The  $r_X$  term was calculated following Norman et al. (1995), which was a function of leaf size, leaf area index, and extrapolated wind speed at the canopy roughness height. The  $r_S$  term was calculated following Kustas and Norman (1999), which weights buoyancy (through  $T_S - T_C$ ) and turbulence (through wind speed extrapolated to the soil surface) using empirical constants. All parameters used in the resistance terms were from previous studies (Kimball et al., 2015; Norman et al., 1995; Kustas and Norman, 1999; and references therein), and none were calibrated in the present study.

Radiometric temperature of the surface ( $T_R$ ) is related to  $T_C$  and  $T_S$  by considering the Stefan-Boltzmann relation:

$$\varepsilon T_R^4 = f_{VR} \varepsilon_C T_C^4 + (1 - f_{VR}) \varepsilon_S T_S^4 \quad (5)$$

where  $\varepsilon$  is the surface emissivity, and  $f_{VR}$  is the view factor of vegetation for the radiometer, such as an infrared thermometer (IRT) or thermal imager, calculated following Colaizzi et al. (2010). Operationally,  $T_R$  is obtained from remotely sensed directional brightness temperature by accounting for surface emissivity and downwelling longwave irradiance from the atmosphere (Norman and Becker, 1995).

Solution of the series resistance network of temperatures is possible using a form of the secant method described by Norman et al. (1995). First, an initial estimate of  $T_C$  (i.e.,  $T_{C,I}$ ) was calculated for non-water-stressed full canopy cover (Jackson et al., 1981):

$$T_{C,I} = T_A + \frac{(R_N - G_0) r_A \gamma^*}{\rho C_P (\Delta + \gamma^*)} - \frac{e_S - e_A}{\Delta + \gamma^*} \quad (6)$$

where  $\Delta$  is the slope of the saturation water vapor pressure-temperature relation ( $\text{kPa } ^\circ\text{C}^{-1}$ ) ( $T_A$  was used in the initial calculation);  $\gamma^* = \gamma(1 + r_c/r_A)$ , where  $\gamma$  is the psychrometric constant ( $\text{kPa } ^\circ\text{C}^{-1}$ ) and  $r_c$  is the bulk canopy resistance ( $\text{s m}^{-1}$ );  $e_S$  and  $e_A$  are the saturation and actual water vapor pressures of the air, respectively ( $\text{kPa}$ ); and all other terms are as defined previously. Initial  $r_c$  values were 50 and  $200 \text{ s m}^{-1}$  for day and night, respectively (Allen et al., 2006), where day was defined as a solar zenith angle less than  $90^\circ$ . It should be noted that this formulation of  $T_{C,I}$  is derived from the Penman-Monteith equation, which differs from the original Norman et al. (1995) formulation that used the Priestley-Taylor equation; both formulations were compared by Colaizzi et al. (2014). In equation 6,  $R_N$  and  $G_0$  were calculated using the FAO 56 method (Allen et al., 1998), which requires  $T_A$  but not  $T_C$  or  $T_S$ . With  $T_R$  and  $T_{C,I}$  known, an initial estimate of  $T_S$  (i.e.,  $T_{S,I}$ ) was obtained by equation 5. Note that  $T_R$  should fall between  $T_C$  and  $T_S$ . Consequently, values of  $f_{VR}$  approaching 1.0 may sometimes lead to  $T_S$  (or  $T_{S,I}$ ) becoming physically too small (if  $T_C > T_R$ ) or too large (if  $T_C < T_R$ ). To avoid unrealistically small values,  $T_S$  (or  $T_{S,I}$ ) was constrained to values equal to or greater than the air wet bulb temperature, which somewhat approximates the minimum temperature expected for the soil, assumed to occur for a wet evaporating surface

(Wanjura and Upchurch, 1996). Unrealistically large  $T_S$  values were avoided by constraining  $LE_S \geq 0$ , as described later. Using  $T_{C,I}$  and  $T_{S,I}$ , initial estimates of  $R_{N,C}$ ,  $r_A$ , and  $r_S$  were obtained;  $r_X$  was calculated beforehand because it did not require  $T_C$  or  $T_S$ . Next,  $T_C$  was approximated by addition of a linear component ( $T_{C,LIN}$ ) and a small correction component ( $\Delta T_C$ ):

$$T_C = T_{C,LIN} + \Delta T_C \quad (7)$$

Expressions for  $T_{C,LIN}$  and  $\Delta T_C$  were derived by Norman et al. (1995) based on the Priestley-Taylor formulation (Priestley and Taylor, 1972); however, Colaizzi et al. (2012d) derived alternative expressions based on the Penman-Monteith formulation (Monteith, 1973) as:

$$T_{C,LIN} = \left\{ \frac{T_A}{r_A} + \frac{T_R}{r_S(1-f_{VR})} + \left[ \frac{r_X \gamma^* R_{N,C}}{\rho C_P (\Delta + \gamma^*)} - \frac{r_X (e_S - e_A)}{r_A (\Delta + \gamma^*)} \right] \left[ \frac{1}{r_A} + \frac{1}{r_S} + \frac{1}{r_X} \right] \right\} \div \left[ \frac{1}{r_A} + \frac{1}{r_S} + \frac{f_{VR}}{r_S(1-f_{VR})} \right] \quad (8a)$$

$$\Delta T_C = \frac{T_R^4 - f_{VR} T_{C,LIN}^4 - (1-f_{VR}) T_{S,LIN}^4}{4 f_{VR} T_{C,LIN}^3 + 4(1-f_{VR}) T_{S,LIN}^3 \left( 1 + \frac{r_S}{r_A} \right)} \quad (8b)$$

where

$$T_{S,LIN} = T_{C,LIN} \left( 1 + \frac{r_S}{r_A} \right) - T_A \frac{r_S}{r_A} - \left[ \frac{r_X \gamma^* R_{N,C}}{\rho C_P (\Delta + \gamma^*)} - \frac{r_X (e_S - e_A)}{r_A (\Delta + \gamma^*)} \right] \left[ 1 + \frac{r_S}{r_A} + \frac{r_S}{r_X} \right] \quad (8c)$$

In equation 8,  $\Delta$  was calculated by replacing  $T_A$  with the average of  $T_A$  and  $T_C$  (or  $T_{C,I}$  if in the initial run) (Lascano and van Bavel, 2007), and  $\gamma^* = \gamma(1 + r_c/r_X)$ . The process was then repeated, where the  $T_C$  value obtained in equation 8 was used to recalculate  $T_S$ ,  $R_{N,C}$ ,  $r_A$ ,  $r_S$ ,  $\Delta$ , and a new  $T_C$ , until the absolute difference of subsequent  $T_C$  values converged to a tolerance or exceeded a maximum number of iterations (we used 0.01 and 100, respectively). If the number of maximum iterations was reached, then  $T_C = T_{C,I}$ . When iteration was complete,  $T_S$  was recalculated, followed by calculation of  $R_{N,S}$ ,  $G_0$ ,  $T_{AC}$ ,  $H_S$ , and  $LE_S$ . This iteration process was slightly different from previous studies (Colaizzi et al., 2012d, 2014), which, in order to reduce model calculation time, did not recalculate available energy and resistance terms for each  $T_C$  iteration. Since  $H = H_C + H_S$ , equation 4 results in:

$$T_{AC} = \frac{\frac{T_A}{r_A} + \frac{T_S}{r_S} + \frac{T_C}{r_X}}{\frac{1}{r_A} + \frac{1}{r_S} + \frac{1}{r_X}} \quad (9)$$

If  $LE_S < 0$ , then condensation on the soil was implied. Although physically plausible at night, it was unlikely during the daytime, especially in semiarid or arid climates. It was more likely that water stress resulted in underestimated  $T_C$ , leading to underestimated  $H_C$  and overestimated  $LE_C$  from equations 4b and 2a, respectively. Further, underestimated  $T_C$  also leads to overestimated  $T_S$  and  $H_S$  from equations 5 and 4c, respectively, and underestimated  $LE_S$  from equation 2b. This case was mitigated by increasing  $r_C$ , relevant variables were recalculated starting with  $T_{C,i}$ , and the process was repeated until  $LE_S \geq 0$ . In the present study, we increased  $r_C$  in increments of 10 up to 1000 s m<sup>-1</sup> (values were chosen arbitrarily). Note that increasing  $r_C$  will increase  $T_C$  and reduce  $T_S$ ; hence, the process of constraining  $LE_S \geq 0$  also reduced the likelihood of unrealistically large  $T_S$  values. When a solution was reached where  $LE_S \geq 0$ , all variables dependent on  $T_C$  were recalculated, and the model run was complete. Note that  $LE_C$  was not constrained from becoming negative in order to allow for possible dew formation on the canopy. Because leaves have a lower heat capacity than soil, nighttime radiative cooling is more likely to cause leaves to fall below dew point temperature compared with soil (Tolk et al., 2006a).

If  $r_C$  reached 1000 s m<sup>-1</sup> and  $LE_S$  was still  $< 0$ , then a dry, non-evaporating soil surface was assumed, which required reformulating the energy balance. In this case,  $LE_S$  was forced to zero, and equation 2b was rewritten as:

$$H_{S,0} = R_{N,S} - G_0 \quad (10)$$

Starting with the previous  $T_C$  value calculated where  $r_C = 1000$  s m<sup>-1</sup>, initial values of  $T_S$ ,  $R_{N,S}$ ,  $G_0$ ,  $H_{S,0}$ ,  $r_A$ , and  $r_S$  were calculated. With  $H_{S,0}$  known, Norman et al. (1995) derived expressions for  $T_{AC}$  for a dry soil surface, again based on the secant method:

$$T_{AC} = T_{AC,LIN} + \Delta T_{AC} \quad (11)$$

where

$$T_{AC,LIN} = \frac{\frac{T_A}{r_A} + \frac{T_R}{r_X f_{VR}} + \frac{H_{S,0}}{\rho C_P} - \frac{H_{S,0} r_S (1 - f_{VR})}{\rho C_P}}{\frac{1}{r_A} + \frac{1}{r_X} + \frac{(1 - f_{VR})}{r_X f_{VR}}} \quad (12a)$$

$$\Delta T_{AC} = \frac{T_R^4 - f_{VR} T_{C,LIN}^4 - (1 - f_{VR}) T_{S,LIN}^4}{4 f_{VR} \left( 1 + \frac{r_X}{r_A} \right) T_{C,LIN}^3 + 4(1 - f_{VR}) T_{S,LIN}^3} \quad (12b)$$

$$T_{C,LIN} = T_{AC,LIN} \left( 1 + \frac{r_X}{r_A} \right) - T_A \frac{r_X}{r_A} - \frac{H_{S,0} r_X}{\rho C_P} \quad (12c)$$

$$T_{S,LIN} = T_{AC,LIN} + \frac{H_{S,0} r_S}{\rho C_P} \quad (12d)$$

Additional details of deriving expressions in equation 12 are provided by Colaizzi et al. (2012d); because these were independent of the Priestley-Taylor or Penman-Monteith formulations, final expressions were unchanged from Nor-

man et al. (1995).

With  $T_{AC}$  calculated,  $T_S$  was calculated by inverting equation 4c, and  $T_C$  was calculated by equation 5, subject to the constraint that  $T_C$  is greater than or equal to its initial value (i.e., when  $r_C = 1000$  s m<sup>-1</sup>). The process was repeated until the absolute difference of subsequent  $T_S$  values converged to a tolerance (0.01 K) or reached a maximum iteration of 100. If the maximum number of iterations was reached, then  $T_S$  was reset to its initial value (i.e.,  $T_C$  when  $r_C = 1000$  s m<sup>-1</sup>); however, this did not occur in the present study. When iteration was complete, all variables dependent on  $T_S$  were recalculated, and the model run was complete.

## METHODS AND MATERIALS

### FIELD MEASUREMENTS

The study was conducted at the USDA-ARS Conservation and Production Research Laboratory in Bushland, Texas (35° 11' N, 102° 6' W, 1170 m above MSL). The climate is classified as semiarid, with mean annual precipitation of 470 mm and Class A pan evaporation of 2600 mm. The climate is noted for strong regional and local advection of sensible heat energy from predominately south and southwest winds during the growing season, with  $H$  contributing up to 60% of  $LE$  for fully irrigated alfalfa (Tolk et al., 2006b). The soil is a Pullman clay loam (fine, mixed, super active, thermic torrertic Paleustolls) (USDA-NRCS, 2015) having slow permeability, a dense B2 horizon from 0.15 to 0.40 m depth, and a calcic horizon from approximately the 1.3 m depth.

All measurements were obtained during BEAREX08 (Evetts et al., 2012a; Kustas et al., 2012b). Upland cotton (*Gossypium hirsutum* L.) was planted on 17 May 2008 at 15.8 plants m<sup>-2</sup> on raised beds with a north-south orientation and spaced 0.76 m apart. Following plant establishment, furrow dikes were installed in the interrows to control runoff and runoff of precipitation and irrigation water (Schneider and Howell, 2000). Irrigation was applied by a hose-fed lateral-move sprinkler system equipped with mid-elevation spray applicators (MESA) (1.5 m above the soil surface) moving in the east-west direction. Irrigations were usually applied in 25 mm events and were scheduled to meet full crop ET, where crop ET was measured by weighing lysimeter and neutron probe (Evetts et al., 2012b).

Measurements of E, T, and ET were obtained by micro-lysimeters, sap flow gauges, and large monolithic lysimeters, respectively. Four large monolithic weighing lysimeters were located in the centers of each of four 4.7 ha fields arranged in a square pattern (designated NE, SE, NW, and SW for northeast, southeast, northwest, and southwest, respectively). All E, T, and ET measurements used in the present study were obtained in the NE field only. Each lysimeter monolith was 3.0 m × 3.0 m on the surface and 2.4 m deep (Marek et al., 1988; Howell et al., 1995). The lysimeters included a load cell and cantilever balance system to measure changes in mass (calibrated to 0.04 mm accuracy in January 2008; Evetts et al., 2012b), where losses were E and T, and gains were irrigation, precipitation, and

dew. The lysimeters were drained by maintaining a -10 kPa vacuum, and drainage effluent was pumped into two tanks suspended from the main lysimeter monoliths, where effluent mass was measured by load cells above each tank. Mass measurements were obtained every 6 s and reported as 15 min averages. Lysimeter measurements were excluded from days where irrigation, precipitation, or personnel were present on the lysimeter (i.e., for soil water or plant measurements, or instrument maintenance and repair), and data were subject to quality control procedures described by Marek et al. (2014).

Microlysimeters were installed approximately 30 m northeast of the NE lysimeter where rows were oriented in the north-south direction. Five microlysimeters were located across the interrow at 0.075, 0.225, 0.375, 0.525, and 0.675 m from the plant row center, west to east, in two replicates (Agam et al., 2012a). The microlysimeters were constructed of white polyvinylchloride (PVC) walls (88 mm deep, 8 mm thick, 105 mm i.d.) and metal bottoms (Evetts et al., 1995). The white PVC walls were designed to minimize lateral heat transfer, and the metal bottoms were designed to avoid impeding vertical heat transfer and avoid drainage (so that changes in mass were due to E only), while containing soil during manual weighing. Each microlysimeter was weighed manually at sunrise and sunset with an electronic scale with a precision of 0.01 mm water equivalent and inside an enclosed box to shelter the scale from wind. Therefore, E measurements spanned ~10 h at night and ~14 h during the day. Immediately after weighing at sunset and at daily intervals, each microlysimeter was replaced with an undisturbed soil core. Replacing soil cores at daily intervals reduced the influence of drainage and root water uptake to be negligible relative to E rates. Microlysimeters were not used during irrigation or precipitation events greater than a few mm.

Heat balance sap flow gauges (Baker and van Bavel, 1987) (models SGA-5 and SGA-9, Dynamax, Inc., Houston, Tex.) were installed on ten cotton plants approximately 30 m northwest of the NE lysimeter. The insulated gauge consisted of a heater strip surrounding the stem, and thermocouples mounted above and below the strip to measure heat fluxes in the xylem and stem. The gauges were installed below the first plant node and approximately 50 mm above the soil surface and heated at ~0.1 W power. The gauges were additionally insulated with layers of bubble wrap and aluminum foil to protect the gauges from changing ambient conditions. Sap flow was converted to T by multiplying average sap flow by the number of instrumented plants per unit area. Measurements were obtained every 5 s from 7:00 to 22:00 CST (15 h duration) and reported as 30 min averages (Agam et al., 2012a).

Micrometeorological measurements were obtained at each lysimeter and at a grass reference site located approximately 250 m east of the lysimeter (Evetts et al., 2012a; Howell et al., 1997, 2000). The grass reference site contained fescue irrigated by subsurface drip and maintained at a height of ~0.12 m. Micrometeorological measurements required by the TSEB model include incoming solar irradiance, wind speed, air temperature, and relative humidity (to calculate water vapor pressure deficit). Incoming solar irra-

diance was measured at the grass reference site with a pyranometer (model PSP, Eppley Laboratories, Newport, R.I.); the other variables were measured at 2 m height primarily at the lysimeter, deployed on a mast outside the north central lysimeter edge. In a few rare instances, missing or suspect micrometeorological data at the lysimeter were substituted with data from the grass reference site (wind speed measured over fescue was adjusted for the greater plant height of cotton following Howell, 1990). Air temperature and relative humidity were measured inside a radiation shield (model HMP45C, Vaisala, Inc., Helsinki, Finland), and wind speed was measured with a cup anemometer (Wind Sentry 03101-5, R.M. Young, Inc., Traverse City, Mich.). Data were measured every 6 s and reported as 15 min averages and were subject to quality control procedures from Allen et al. (1998).

Directional brightness temperature ( $T_B$ ) was measured by two infrared thermometers (model IRT/C.5-T-80F/27C, Exergen Corp., Watertown, Mass.). The IRTs were deployed approximately 22 m northeast of the NE lysimeter and 8 m south of the microlysimeters; they viewed the plant canopy directly overhead at nadir and at a 1.5 m height from a stationary mast to the north. Each IRT consisted of a type-T thermocouple, germanium lens, 8 to 14  $\mu\text{m}$  bandwidth, factory-calibrated range of 0°C to 50°C, internal emissivity setting of 1.0, and 5:1 field of view, resulting in a 0.30 m diameter footprint at the soil surface (Colaizzi et al., 2010). The IRTs were enclosed in white PVC to insulate the detector and internal body and reduce measurement error caused by longwave variability; relative performance of the TSEB model using IRTs with and without detector temperature correction was discussed by Colaizzi et al. (2012a). The IRT lenses were cleaned each morning and inspected for correct viewing angle using a laser mounted in a jig that was lathed to fit in the barrel in front of the IRT lens. Data were excluded during the times of lens cleaning and inspection, and if  $T_B$  replicates deviated from each other by more than 1°C at dawn (Wanjura et al., 2004).  $T_B$  was sampled every 6 s and reported as 15 min averages of the two IRTs. Average  $T_B$  was converted to  $T_R$  (for input to eq. 5) by accounting for surface emissivity ( $\epsilon$ ) and reflected downward hemispherical longwave radiation from the atmosphere:

$$T_R^4 = \frac{\epsilon_R}{\epsilon} T_B^4 + \left(1 - \frac{1}{\epsilon}\right) \epsilon_{atm} T_A^4 \quad (13)$$

where  $\epsilon_R$  is the target emissivity that is set in the radiometer firmware,  $\epsilon_{atm}$  is the hemispherical longwave atmospheric emissivity, and all other terms are as defined previously. Soil ( $\epsilon_S$ ) and canopy ( $\epsilon_C$ ) emissivities were both assumed 0.98 (Idso et al., 1969; Campbell and Norman, 1998);  $\epsilon_S$  was verified by a multiband thermal radiometer (model CE 312, Cimel Electronique, Paris, France) measurements over bare soil. With  $\epsilon_S$  and  $\epsilon_C$  equal,  $\epsilon$  was also assumed 0.98. Longwave reflectance was calculated as the complement of  $\epsilon$  (i.e., 0.02), and  $\epsilon_{atm}$  was calculated for the full longwave spectrum for clear skies using the equation of Idso (1981):

$$\varepsilon_{atm} = 0.70 + 5.95 \times 10^{-4} e_A \exp\left(\frac{1500}{T_A}\right) \quad (14)$$

where  $T_A$  has units of K, and other terms are as defined previously.

Soil heat flux at the surface ( $G_0$ ) was determined by the calorimetric correction method using measurement arrays of heat flux, soil temperature, and volumetric soil water content located a few meters from the microlysimeter site (Agam et al., 2012b; Evett et al., 2012c). Briefly, instrument arrays were deployed across the interrow similar to the microlysimeters, in two replicates of five locations 0.085, 0.235, 0.385, 0.535, and 0.685 m west to east from the plant row center. Soil temperature was measured by type-T thermocouples constructed in-house of copper constantan wire (EXPP-T-20-TWSH wire, Omega Engineering, Inc., Stamford, Conn.) and buried at 0.02 and 0.06 m depths. Volumetric soil water content was measured with a time-domain reflectometry (TDR) system, also constructed in-house and described by Evett (2000a, 2000b) and Evett et al. (2005, 2012c). Trifilar TDR probes were also buried at 0.02 and 0.06 m depths. Soil heat flux below the surface was measured by soil heat flux plate flow transducers (model HFT-3.1, Radiation and Energy Balance Systems, Inc., Bellevue, Wash.) buried at 0.08 m depth. The calorimetric correction method included dividing the soil into two layers (0 to 0.04 m and 0.04 to 0.08 m depths) and calculating soil heat flux divergence in these two layers. The  $G_0$  obtained by calorimetric correction was averaged across the five interrow locations and two replicates and reported as 30 min intervals.

Plant width ( $w_C$ ) and plant height ( $h_C$ ) were measured daily at the IRT and microlysimeter sites and approximately weekly at the lysimeters. Leaf area index (LAI) was obtained at key cotton growth stages by destructive plant samples from three 1.0 m<sup>2</sup> locations in the lysimeter field that were sufficiently distant from the lysimeters and instrumented sites. The destructive plant samples included  $w_C$  and  $h_C$  measurements prior to plant removal; leaves were stripped, leaf area was measured with a leaf area meter (model LI-3100, LI-COR, Lincoln, Neb.), and LAI was calculated. The leaf area meter was calibrated using a reference disk of 0.005 m<sup>2</sup> area. The  $w_C$ ,  $h_C$ , and LAI values were interpolated between measurement dates by growing degree days of cotton (15.6°C base temperature).

#### MODEL EVALUATION

The TSEB model was evaluated by comparing calculated values of  $R_N$ ,  $G_0$ ,  $LE$ ,  $E$ ,  $T$ , and  $ET$  to measurements. First, energy fluxes were calculated by the TSEB model, averaged over 15 min time steps. Calculated  $G_0$  was averaged to 30 min time steps for comparison with measurements. Calculated  $LE_S$ ,  $LE_C$ , and  $LE$  (W m<sup>-2</sup>) were converted to  $E$ ,  $T$ , and  $ET$ , respectively (mm per 15 min); for example:

$$ET = LE \frac{1000 \times 900}{(10^6 \rho_w \lambda)} \quad (15)$$

where 1000 converts m to mm, 900 converts time intervals

of 1.0 s to 15 min,  $10^6$  converts MJ to J,  $\rho_w$  is the density of water at 20°C (1000 kg m<sup>-3</sup>), and  $\lambda$  is the latent heat of vaporization (MJ kg<sup>-1</sup>), where  $\lambda = 2.501 - 0.002361T_A$ , and  $\lambda = \sim 2.44$  MJ kg<sup>-1</sup> during the daytime at the study location. For conversion to  $E$  and  $T$  using equation 15,  $LE$  was substituted with  $LE_S$  and  $LE_C$ , respectively. Calculated  $E$  and  $T$  were summed to the appropriate measurement interval (i.e., 10 and 14 h for nighttime and daytime  $E$ , respectively, and 30 min and 15 h for  $T$ ); calculated and measured  $ET$  were summed to 24 h (midnight to midnight) values.

The discrepancy between calculated and measured variables was evaluated in terms of the index of model agreement (IOA), root mean square error (RMSE), mean absolute error (MAE), and mean bias error (MBE). The IOA is a first-order variant of the Nash-Sutcliffe coefficient of model efficiency (Nash and Sutcliffe, 1970), which was advocated by Legates and McCabe (1999) because the first-order formulation was less sensitive to outliers compared with higher orders. Similar to the Nash-Sutcliffe model efficiency, the IOA varies from  $-\infty$  to 1.0, where IOA = 1.0 indicates perfect agreement between calculated and measured values, and IOA = 0 indicates that the calculated values contain no more information than the mean of all measured values. The extent that RMSE > MAE indicates outliers in calculated versus measured scatter, which may have further utility in model diagnostics (Legates and McCabe, 1999).

## RESULTS AND DISCUSSION

### CANOPY COVER VARIATION

Cotton plant establishment was delayed due to unfavorable growing conditions for several weeks following planting. When plants were at cotyledon stage, afternoon  $T_A$  frequently exceeded 35°C, wind gusts exceeded 15 m s<sup>-1</sup>, and reference  $ET$  for a short crop ( $ET_{os}$ ) exceeded 10 mm d<sup>-1</sup> (data not shown). The large atmospheric demand required frequent irrigation to ensure seed germination; however, more frequent irrigations resulted in more severe soil crusting. This in turn favored laminar wind flow near the soil surface, and cotyledons were abraded by wind-blown soil particles. Growing conditions were more favorable after approximately DOY 178 for the remainder of the 2008 growing season, and plants damaged by wind-blown soil eventually recovered. However, spatial variability of plant growth and development was larger than expected from early to mid-season.

Spatial variability of plant growth and development was qualitatively assessed in the NE lysimeter field during the 2008 growing season (fig. 2). During rapid growth approximately from DOY 212 to 240, canopy width (fig. 2a) and height (fig. 2b) were larger at the NE lysimeter and IRT site compared with the three sample locations in the NE field where destructive plant samples were obtained to determine LAI. At other times, canopy width and height was less variable throughout the measurement locations. Spatial variability of LAI was largest around DOY 240 (from  $\sim 2.5$  to  $\sim 3.5$  m<sup>2</sup> m<sup>-2</sup>), just prior to the start of leaf senescence when LAI decreased (fig. 2c). Although LAI would be expected

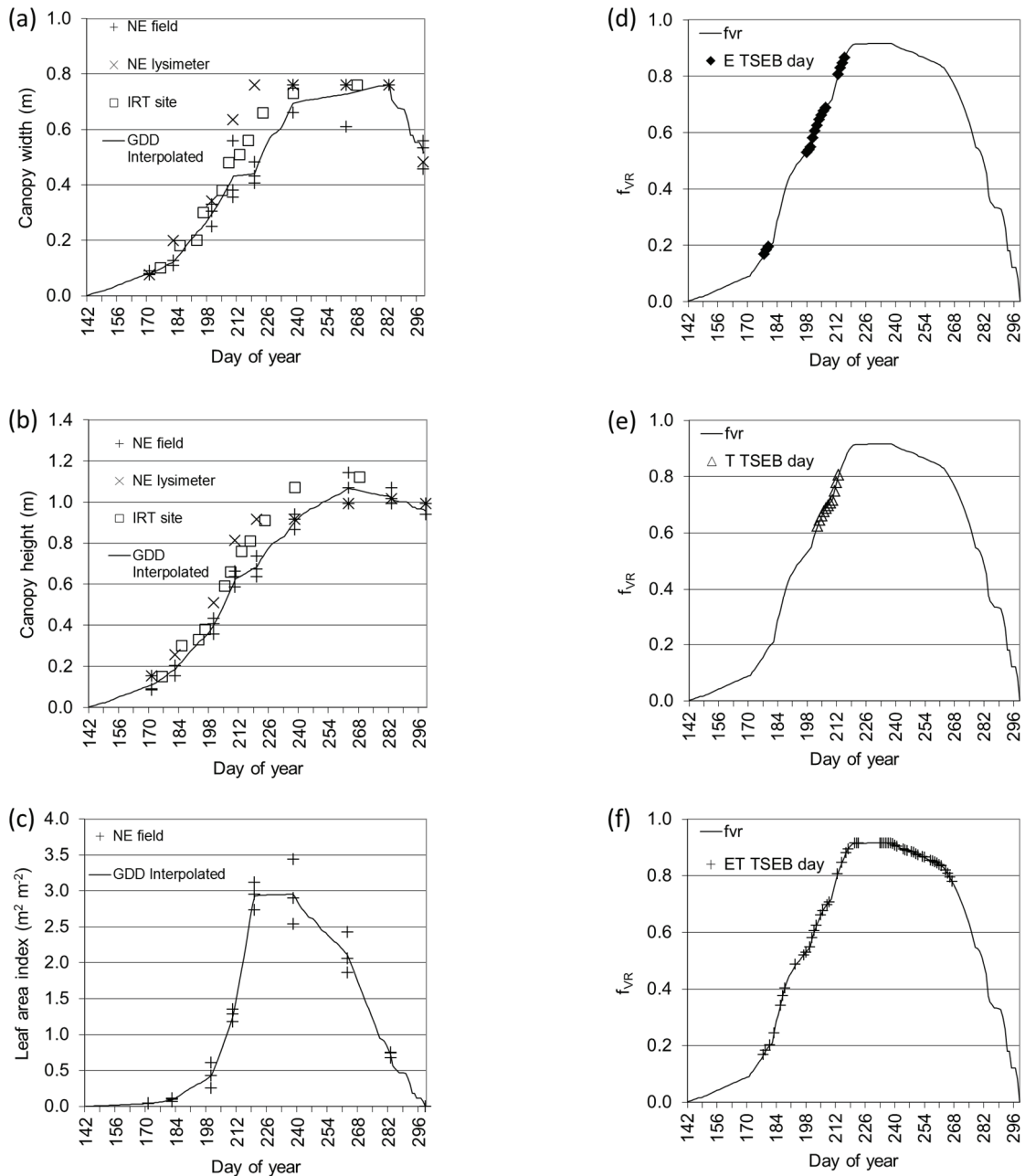


**Figure 2.** Cotton plant measurements and interpolated values based on growing degree days (GDD) during BEAREX08 of (a) canopy width, (b) canopy height, (c) leaf area index, and vegetation-radiometer view factor ( $f_{VR}$ ) on TSEB test days for (d) evaporation (E), (e) transpiration (T), and (f) evapotranspiration (ET) (Colaizzi et al., 2012d, 2014).

to be larger at the NE lysimeter and IRT site compared with the NE field from DOY 212 to 240, LAI was not adjusted upward for these sites. Therefore, at least some discrepancy between measured and calculated energy fluxes could be attributed to plant spatial variability in canopy width, canopy height, and LAI (Kustas et al., 2012a).

A fundamental objective of the present study was to investigate E and T partitioning by the TSEB model over a wide range of vegetation cover. This was done by considering variation in  $f_{VR}$ , which was dependent on canopy width, height, and LAI (fig. 2). The days on which measurements of E, T, and ET were available to test the TSEB model were denoted by symbols on the  $f_{VR}$  line (figs. 2d, 2e, and

2f, respectively). Measurements of E were obtained from DOY 178 to 215 but in three separate intensive observation periods (Agam et al., 2012a); this spanned a relatively large range of  $f_{VR}$  (0.17 to 0.85). However, T measurements were obtained only from DOY 204 to 213, spanning a smaller range of  $f_{VR}$  (0.63 to 0.80). Although sap flow gauges are perhaps the most direct method to measure T (Sutanto et al., 2014), successful measurement of T is contingent on maintaining thermal continuity between the heater strip and the plant stem. The gauge design limits the range of stem diameters on which gauges can be used. In this research, gauges were not available for early season measurements. Measurements of ET used in the present study were ob-

tained from DOY 178 to 267;  $f_{VR}$  increased from 0.17 to 0.92 and then decreased to 0.78. Although a wider range of vegetation cover would have been desirable for T measurements, few TSEB model studies have included both E and ET measurements from sparse to full canopy cover.

#### MEASURED AND CALCULATED DISCREPANCIES

Discrepancies between calculated and measured variables were quantified in terms of IOA, RMSE, MAE, and MBE (table 1) and plot (fig. 3). Refinements to the TSEB model used in the present study resulted in all calculated vs. measured variables having IOA > 0.50. For instantaneous energy fluxes ( $R_N$ ,  $G_0$ , and  $LE$ ), RMSE was <65 W m<sup>-2</sup> and |MBE| was <12 W m<sup>-2</sup>. For depth variables (E, T, and ET), RMSE was <0.9 mm and |MBE| was <0.5 mm. For all variables, RMSE/MAE was <1.64, implying that calculated vs. measured discrepancies were relatively free of outliers (Legates and McCabe, 1999).

The largest discrepancies were calculated vs. measured E and summed (15 h) T, with IOA of 0.78 and 0.52, respectively; IOA for all other variables were >0.80 (table 1). Measured nighttime E was <0.01 to 0.34 mm, and measured daytime E was 1.0 to 2.7 mm (fig. 3e; see also Agam et al., 2012a, table 1). Agam et al. (2012a) found no significant correlations between 24 h E and lysimeter ET ( $r^2 = 0.35$ ) or calculated alfalfa reference ET ( $r^2 = 0.13$ ) and surmised that E was decoupled from atmospheric demand due to interactions with  $h_C$  and LAI during rapid canopy development when E was measured. However, they pointed out that for low to moderate wind speeds (i.e., ~1 to 4 m s<sup>-1</sup>), E was responsive to wind direction relative to crop row, with greater E associated with wind directions more parallel to the crop row. Hence, they recommended that E be further explored in terms of the interaction between row orientation, climate variables, and overall energy balance. Measured T in 30 min intervals ( $T_{30}$ ) was approximately 0.0 to 0.5 mm (fig. 3d), and 15 h sums were 5.2 to 8.3 mm (fig. 3e). Since T measurements were available for only a small range of canopy cover and daily atmospheric demand, a limited range of 15 h T measurements would be expected. Nonetheless, RMSE and MAE were larger for T relative to E and ET, as seen by the larger scatter. The E and T discrepancies were substantially smaller using the Penman-Monteith version of the TSEB compared with the Priestley-Taylor version, where the latter over- and underestimated E and T, respectively, by up to ~5 mm (Colaizzi et al., 2014).

The 24 h sums of measured ET ranged from 3.2 to 14.4 mm, which reflected the relatively large range of atmospheric demand and vegetation cover when ET meas-

urements were obtained (fig. 3f). Discrepancies with calculated ET values resulted in IOA = 0.87 and RMSE, MAE, and MBE of 0.63, 0.49, and -0.31 mm d<sup>-1</sup>, respectively (table 1). In a concurrent study during BEAREX08, Anderson et al. (2012) calculated  $LE$  using a TSEB version based on the clumping index and Priestley-Taylor equation; their study included  $T_R$  retrieval using measurements of upwelling hemispherical longwave radiation. Their RMSE, MAE, and MBE were 0.74, 0.57, and 0.24 mm d<sup>-1</sup>, respectively (converted from MJ m<sup>-2</sup> d<sup>-1</sup> reported in their table 2) relative to NE lysimeter measurements. French et al. (2015) also used the clumping index and Priestley-Taylor version of the TSEB model, but  $T_R$  measurements were obtained with an airborne thermal imager, and ET measurements were derived from a soil water balance, where soil water content was measured by neutron probe. Their study included two seasons of cotton, for which RMSE was 0.5 and 1.6 mm d<sup>-1</sup> and MBE was -0.2 and -0.6 mm d<sup>-1</sup>. The similar discrepancies of measured and calculated  $LE$  or ET using the Priestley-Taylor version would suggest no justification for the Penman-Monteith version; however, the main advantage of the latter has been in E and T partitioning.

Refinements to the TSEB model used in the present study resulted in similar, and in a few cases slightly improved, results compared with previous model versions (Colaizzi et al., 2012d, 2014). To review, model refinements included a new method to calculate  $G_0$  (eq. 3), use of the Richardson number instead of the Monin-Obukhov length for stability correction in  $r_A$ , use of the ASHRAE equation to calculate  $r_A$  in the rare case (at the Bushland site) of small (<1.0 m s<sup>-1</sup>) wind speeds, replacing  $T_A$  with the average of  $T_A$  and  $T_C$  for  $\Delta$ , and recalculating all available energy and resistance variables during each  $T_C$ ,  $T_S$ , and  $T_{AC}$  iteration. Although the Richardson number eliminated an additional iteration within the  $r_A$  function, this appeared to have been offset by the additional calculations in the temperature iterations, with no noticeable change in the total model calculation time requirement. Nonetheless, these changes were deemed as having greater rigor compared with previous TSEB model versions, which may reduce instances of the model failing to converge to physically realistic solutions (Kimball et al., 2015). Furthermore, the present TSEB model was tested for a limited set of conditions because few, if any, studies included the measurements required to investigate E and T partitioning. Hence, model refinements should be tested under a wider range of conditions, such as other crops, different irrigation systems (e.g., sprinkler and microirrigation), and limited or no irrigation.

**Table 1. Statistical parameters of discrepancy between measured and calculated net radiation ( $R_N$ ), surface soil heat flux ( $G_0$ ), latent heat flux ( $LE$ ), 30 min transpiration ( $T_{30}$ ), day or night evaporation (E), day and evening transpiration (T), and summed 24 h evapotranspiration (ET). See figure 3 for scatter plots.**

Variable	Units	<i>n</i>	Measured		Calculated		IOA	RMSE	MAE	MBE
			Mean	SD	Mean	SD				
$R_N$	W m <sup>-2</sup>	5088	161	238	149	250	0.95	27.4	21.8	-11.7
$G_0$	W m <sup>-2</sup>	1175	6.5	51.2	7.4	51.4	0.89	12.5	8.8	0.91
$LE$	W m <sup>-2</sup>	5088	203	231	194	237	0.88	65.0	46.2	-8.6
$T_{30}$	mm 0.5 h <sup>-1</sup>	330	0.23	0.14	0.24	0.15	0.84	0.059	0.042	0.010
E	mm	22	0.94	0.90	0.74	0.74	0.78	0.54	0.33	-0.19
T	mm	11	6.9	1.0	7.2	0.82	0.52	0.87	0.69	0.31
ET	mm d <sup>-1</sup>	53	7.2	2.3	6.9	2.5	0.87	0.63	0.49	-0.31

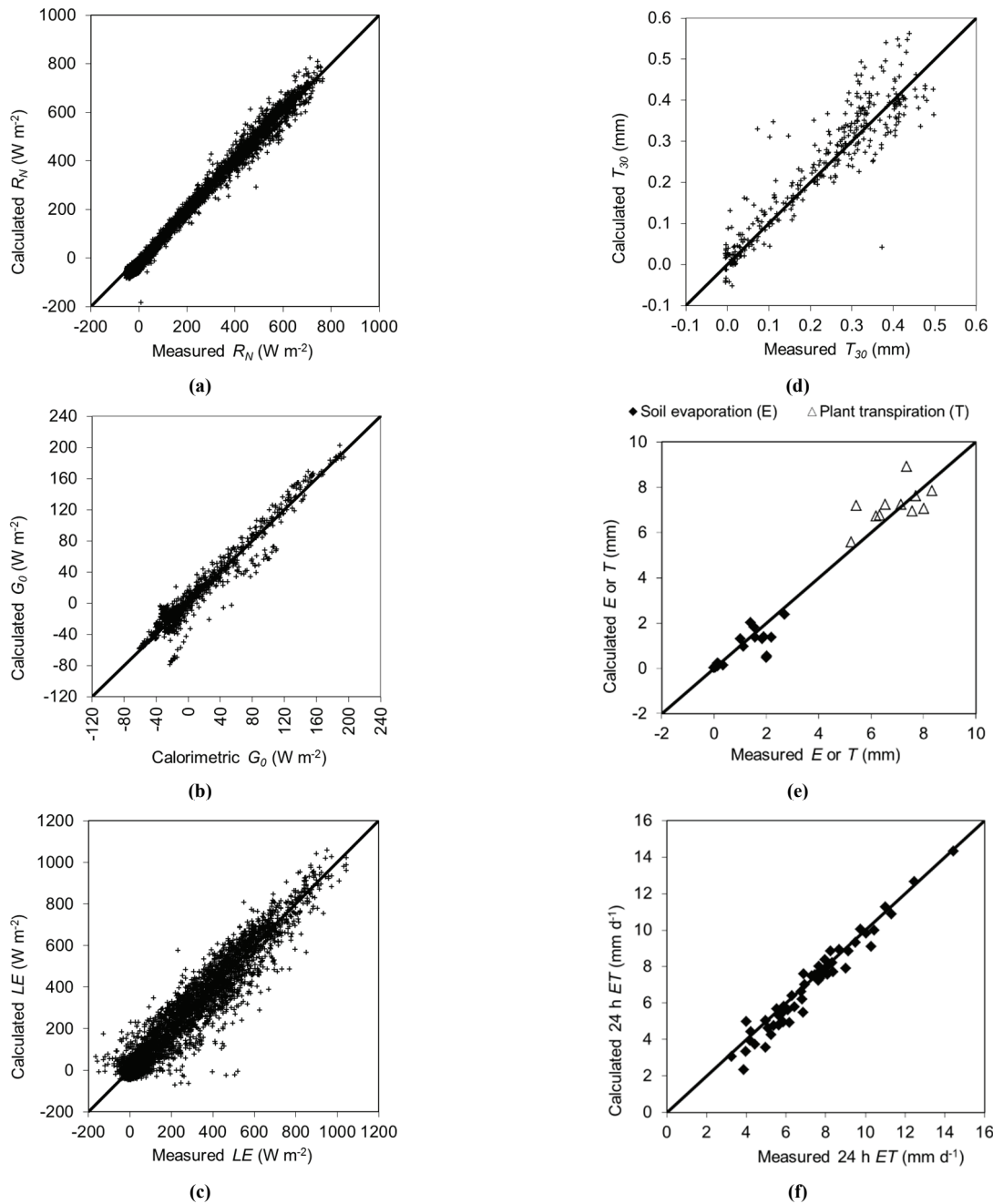


Figure 3. Scatter plots of calculated vs. measured (a) net radiation ( $R_N$ ), (b) surface soil heat flux ( $G_0$ ), (c) latent heat flux ( $LE$ ), (d) 30 min transpiration ( $T_{30}$ ), (e) day or night evaporation ( $E$ ) and day and evening transpiration ( $T$ ), and (f) summed 24 h evapotranspiration ( $ET$ ). See table 1 for statistical parameters of discrepancy. The solid line is 1:1 agreement.

#### VARIATION OF FINAL BULK CANOPY RESISTANCE

The bulk canopy resistance ( $r_C$ ) was a convenient method to partition available energy for the initial estimates of  $LE_C$  and  $T_C$  in the Penman-Monteith TSEB version, independently of the series resistances (fig. 1). (The  $\alpha_{PT}$  factor was the equivalent partitioning method in the Priestley-Taylor TSEB version; see Colaizzi et al., 2014, for a comparison of TSEB model versions). Initial estimates of  $LE_C$  and  $T_C$  assumed non-water-stressed conditions where atmospheric demand was the limiting factor. The initial  $r_C$  values were assumed 50 and 200  $s\ m^{-1}$  for day and night, respectively, after Allen et al. (2006). If solution of the en-

ergy balance using the secant method resulted in  $LE_S < 0$ , then it was implied that  $LE_C$  and/or  $LE_S$  were limited by factors other than atmospheric demand. Therefore,  $r_C$  was increased in 10  $s\ m^{-1}$  increments, up to 1000  $s\ m^{-1}$ , in the Penman-Monteith TSEB version (or  $\alpha_{PT}$  incrementally decreased in the Priestley-Taylor TSEB version) to reduce  $LE_C$  and increase  $T_C$ , until  $LE_S \geq 0$  (or  $LE_S$  is forced to zero). The iterative approach used here in effect accommodates variation of  $r_C$ , which although it differs from other variable  $r_C$  approaches, may implicitly account for  $r_C$  being responsive to linkages between micrometeorological variables and plant physiology, even under non-water-stressed

conditions (e.g., Lascano and van Bavel, 2007). Questions then arise as to what extent, if any, did final  $r_C$  values vary, and were variations related to plant growth stage, time of day, or measured energy fluxes?

Final  $r_C$  values were substantially variable and frequently exceeded the initial 50 (day) and 200  $s\ m^{-1}$  (night) values (fig. 4). Variable  $r_C$  was not related to canopy cover or time in the growing season (data not shown) but was clearly related to time of day (fig. 4a). At night,  $r_C$  tended to exceed 200  $s\ m^{-1}$  more frequently before midnight and less frequently after midnight. This suggested that a greater proportion of available energy was partitioned to  $LE$  after midnight, which might have been related to upward movement of water vapor in the soil making more water available near the soil surface compared with before midnight (Idso et al., 1974; Novak, 2010). During morning hours between 8:00 and 12:00 CST, all  $r_C$  values were  $<200\ s\ m^{-1}$  and seldom exceeded 100  $s\ m^{-1}$ ; during the afternoon from approximately 12:00 to sunset,  $r_C$  was mostly between 50 and 200  $s\ m^{-1}$ , with a few exceptions exceeding  $\sim 200\ s\ m^{-1}$ . Available energy would be expected to be greater during the afternoon compared with morning hours due to larger  $T_A$ , larger water vapor pressure deficit, and larger wind speed (although shortwave irradiance was sometimes moderated by afternoon clouds); larger  $r_C$  values would again imply greater partitioning of available energy to  $H$  and less to  $LE$  compared with morning hours. In some cases, advected

energy resulted in  $H < 0\ W\ m^{-2}$ , but these most frequently occurred during afternoon hours, and  $r_C \sim 50\ s\ m^{-1}$ . At the other extreme, a few cases resulted in  $r_C = 1000\ s\ m^{-1}$ , requiring  $LE_S$  to be forced to zero; with a few exceptions, this occurred outside of 8:00 to 16:00 CST when available energy was relatively limited.

From the distribution of final  $r_C$  as related to time of day, it was expected that the distribution of final  $r_C$  was inversely related to measured  $LE$  (here,  $LE$  was converted from lysimeter mass measurements by inverting eq. 15) (fig. 4b). Minimum daytime  $r_C$  values (50  $s\ m^{-1}$ ) occurred for nearly the entire range of measured  $LE$ , but maximum  $r_C$  values were asymptotically related to  $LE$ . Negative  $LE$  was measured in a few instances; these were related to dew formation and light rainfall events that were too small to be registered by the rain gauge but still detected as an increase in mass by the lysimeter (Colaizzi et al., 2014). Available energy ( $R_N - G_0$ ) did not exceed  $\sim 700\ W\ m^{-2}$ ; therefore, larger  $LE$  included advected energy (Tolk et al., 2006b). The final  $r_C$  values as related to independent  $LE$  measurements lend further support for the iterative secant procedure in implicitly accounting for  $r_C$  variation.

The calculated and measured differences in  $T_C$  (fig. 4c) and  $LE$  (fig. 4d) were also related to final  $r_C$  (see Colaizzi et al., 2012d, for description of  $T_C$  measurements). The largest discrepancies, both positive and negative, resulted

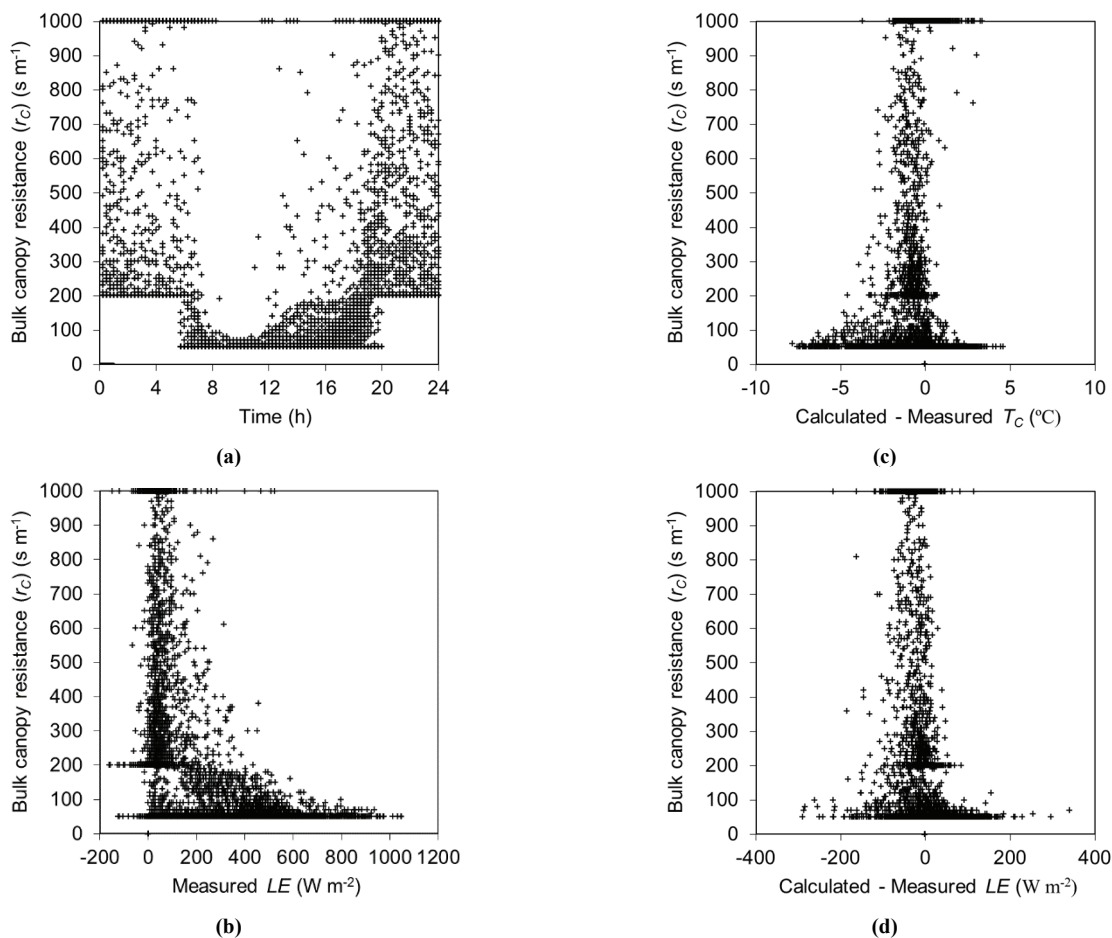


Figure 4. Final bulk canopy resistance ( $r_C$ ) vs. (a) time, (b) latent heat flux ( $LE$ ), (c) calculated – measured canopy temperature ( $T_C$ ), and (d) calculated – measured  $LE$ .

when final  $r_c$  tended toward minimum values, and to a lesser extent when  $r_c$  reached  $1000 \text{ s m}^{-1}$  (i.e., when  $LE_S$  was forced to zero). Positive  $T_C$  and negative  $LE$  discrepancies implied that  $r_c$  was too large, and that values of  $r_c < 50 \text{ s m}^{-1}$  (day) or  $r_c < 200 \text{ s m}^{-1}$  (night) may have been more appropriate, such as when soil was in stage 1 drying. The opposite case (i.e., negative  $T_C$  and positive  $LE$  discrepancies) implied that  $r_c$  values were too small and should have been increased further, resulting in greater partitioning of energy to  $LE_S$  (e.g., soil in stage 1 drying) and less to  $LE_C$ , or greater energy to  $H$  and less to  $LE$ . Discrepancies approached zero for the entire range of  $r_c$  values but became closer to zero with increasing  $r_c$  values up to  $1000 \text{ s m}^{-1}$ . This implied that discrepancies were likely to become smaller as limits were imposed to  $LE_S$  or  $LE_C$ . These limits might include advanced drying of soil (e.g., stage 2) or transpiration falling below atmospheric demand.

The range of  $r_c$  values in figure 4 was much larger than the ranges assumed or reported by other studies, such as Allen et al. (1998, 2005, 2006), Lascano et al. (2010), and Idso (1983). Allen et al. (2006) derived  $r_c$  for well-watered fescue at various locations in the U.S. and Spain, where  $r_c$  was derived from weighing lysimeter measurements of ET, and measured ET was used in the ASCE Standardized Penman-Monteith equation described by Allen et al. (2005) to solve for  $r_c$ . The fescue was maintained at heights of  $\sim 0.12$  to  $0.23 \text{ m}$ , and resulting  $r_c$  ranged from  $\sim 25$  to  $150 \text{ s m}^{-1}$  during the daytime ( $\sim 8:00$  to  $20:00$  local time). The larger  $r_c$  values were early and late in the day, and the minimum values were at midday, which would be expected, as stomatal resistances are larger at night and smaller during the day. Allen et al. (2006) concluded that the resulting  $r_c$  behavior lent support for the use of constant  $r_c$  values for daily ( $70 \text{ s m}^{-1}$ ), daytime ( $50 \text{ s m}^{-1}$ ), and nighttime ( $200 \text{ s m}^{-1}$ ) time periods in the FAO 56 (Allen et al., 1998) and ASCE Standardized (Allen et al., 2005) Penman-Monteith equations used to calculate ET for a grass reference crop. In a similar manner, Lascano et al. (2010) derived  $r_c$  for well-watered alfalfa maintained at heights of  $0.29$  to  $0.67 \text{ m}$  from ET measured by weighing lysimeters at Bushland, Texas. However, their ET model was the recursive combination method (RCM), which, unlike the FAO 56 or ASCE Standardized Penman-Monteith equations, made no assumptions about the surface temperature or surface vapor pressure. Using a single day, they fit  $r_c$  values to a second-order polynomial as a function of time of day and used the  $r_c$  function to calculate ET for other days. Resulting  $r_c$  values ranged from  $\sim 20$  to  $80 \text{ s m}^{-1}$ . Note that  $r_c$  derived in this way depends on the ET model used, along with the methods used to calculate or measure variables used within in the ET model, such as  $r_A$  and stability correction (if used). Idso (1983) showed that leaf stomatal conductance measured by a porometer was a strong linear function of  $R_N$  measured by a net radiometer for fig trees, lettuce, and wheat. Although the porometer measurements were at the leaf rather than the canopy scale, the stomatal resistance (reciprocal of conductance) values for wheat, for example, ranged from  $50$  to  $125 \text{ s m}^{-1}$  for  $R_N$  values from  $800$  to  $300 \text{ W m}^{-2}$ , respectively, which were similar in magnitude to  $r_c$  found by Allen et al. (2006) and Lascano et al. (2010).

Both the intent and the calculation methods of the  $r_c$

values in figure 4 were different from those reported in other studies. Here,  $r_c$  values ( $50$  and  $200 \text{ s m}^{-1}$  for day and night, respectively) were used to initialize  $T_C$  and  $LE_C$  in the TSEB model, where the initial conditions were assumed to be free of water stress. The  $r_c$  values were allowed to increase up to  $1000 \text{ s m}^{-1}$  (the exact upper limit did not impact TSEB model convergence; data not shown) until equations 7 and 8 were overridden and replaced with equations 8 to 12 where  $LE_S = 0$  was assumed. Thus, the larger range of  $r_c$  shown here was the result of the iterative process used in the TSEB model, in contrast to other studies where  $r_c$  was derived from stomatal or ET measurements. However, the larger  $r_c$  values shown here may have also been related to the much larger range of vegetation cover and LAI earlier in the season, and the inclusion of ET calculation and measurement days later in the season when cotton leaves began to senesce (fig. 2).

## SUMMARY AND CONCLUSIONS

The TSEB model was tested using measurements of  $R_N$ ,  $G_0$ ,  $LE$ ,  $E$ ,  $T$ , and  $ET$  obtained over fully irrigated cotton having a wide range of canopy cover during BEAREX08. Measurements of  $E$ ,  $T$ , and  $LE/ET$  were obtained by micro-lysimeter, sap flow gauge, and weighing lysimeter, respectively. Relatively few studies have tested the TSEB using weighing lysimeters, and still fewer studies also included separate  $E$  and  $T$  measurements, which are required to assess  $E$  and  $T$  partitioning by the model. Hence, BEAREX08 resulted in unique data for soil-plant-atmosphere energy balance studies, which led to several significant changes in the TSEB model.

Previous versions of the TSEB model accounted for non-random spatial distribution of vegetation, such as occurs in row crops, using an empirically based clumping index approach. Further, initial values of  $LE_C$  and  $T_C$ , along with calculation of temperatures using a form of the secant method, were based on the Priestley-Taylor equation. Following BEAREX08, the clumping index was replaced with a geometric model that used three canopy view factors and elliptical hedgerows to represent row crop canopies. In addition, equations derived from the Priestley-Taylor ET model were replaced with equations derived from the Penman-Monteith model. Both changes resolved incorrect  $E$  and  $T$  partitioning, which were previously shown to be over- and underestimated, respectively, by up to  $5 \text{ mm}$ . More recent TSEB refinements described herein included developing a new  $G_0$  model, replacing the Monin-Obukhov length with the Richardson number for stability correction in  $r_A$ , use of the ASHRAE equation based on buoyancy to calculate  $r_A$  during wind speeds of  $< 1.0 \text{ m s}^{-1}$ , calculating  $\Delta$  using the mean of  $T_A$  and  $T_C$  (instead of  $T_A$  only), and recalculating all temperature-dependent terms at each model iteration. These recent refinements only marginally improved TSEB performance but nonetheless improved rigor and may reduce the likelihood of the model failing to converge to physically plausible solutions. The variation and distribution of  $r_c$  was strongly related to time of day and measured  $LE$ , with  $r_c$  exceeding baseline values (i.e.,  $50$

and 200 s m<sup>-1</sup> during daytime and nighttime, respectively) more frequently from approximately noon until midnight and also when *LE* was relatively smaller.

The present study tested the TSEB model, specifically addressing E and T partitioning over a wide range of vegetation cover. However, conditions were limited to fully irrigated cotton where water stress was minimized. The need is urgent to conduct similar studies for different crops, for limited or no irrigation where water stress is more prevalent, and for different irrigation systems, such as sprinkler and microirrigation, which are being increasingly adopted worldwide in place of gravity irrigation. Simultaneous measurements of E, T, and ET remain challenging but will be of increasing importance in finding ways to increase the T/ET ratio and increase crop water productivity.

#### ACKNOWLEDGEMENTS

This research was supported by USDA-ARS National Program 211, Water Availability and Watershed Management, and in part by the Ogallala Aquifer Program, a consortium of the USDA Agricultural Research Service, Kansas State University, Texas AgriLife Research, Texas AgriLife Extension Service, Texas Tech University, and West Texas A&M University. We thank the numerous biological technicians and student workers for their meticulous and dedicated efforts in executing experiments and obtaining and processing data.

#### REFERENCES

- Agam, N., Kustas, W. P., Anderson, M. C., Li, F., & Colaizzi, P. D. (2007). Utility of thermal sharpening over Texas High Plains irrigated agricultural fields. *J. Geophys. Res.*, *112*, D19110. <http://dx.doi.org/10.1029/2007jd008407>.
- Agam, N., Evett, S. R., Tolk, J. A., Kustas, W. P., Colaizzi, P. D., Alfieri, J. G., McKee, L. G., Copeland, K. S., Howell, T. A., & Chávez, J. L. (2012a). Evaporative loss from irrigated interrows in a highly advective semi-arid agricultural area. *Adv. Water Resour.*, *50*, 20-30. <http://dx.doi.org/10.1016/j.advwatres.2012.07.010>.
- Agam, N., Kustas, W. P., Evett, S. R., Colaizzi, P. D., Cosh, M., & McKee, L. G. (2012b). Soil heat flux variability influenced by row direction in irrigated cotton. *Adv. Water Resour.*, *50*, 31-40. <http://dx.doi.org/10.1016/j.advwatres.2012.07.017>.
- Alfieri, J. G., Kustas, W. P., Prueger, J. H., Hipps, L. E., Evett, S. R., Basara, J. B., Neale, C. M. U., French, A. N., Colaizzi, P., Agam, N., Cosh, M. H., Chavez, J. L., & Howell, T. A. (2012). On the discrepancy between eddy covariance and lysimetry-based surface flux measurements under strongly advective conditions. *Adv. Water Resour.*, *50*, 62-78. <http://dx.doi.org/10.1016/j.advwatres.2012.07.008>.
- Allen, R. G., Pereira, L. S., Raes, D., & Smith, M. (1998). Crop evapotranspiration: Guidelines for computing crop water requirements. Irrigation and Drainage Paper No. 56. Rome, Italy: United Nations FAO.
- Allen, R. G., Walter, I. A., Elliott, R. L., Howell, T. A., Itenfisu, D., Jensen, M. E., & Snyder, R. L. (2005). The ASCE standardized reference evapotranspiration equation. ASCE/EWRI Task Committee Report. Reston, Va.: ASCE.
- Allen, R. G., Pruitt, W. O., Wright, J. L., Howell, T. A., Ventura, F., Snyder, R., Itenfisu, D., Steduto, P., Berengena, J., Yrisarry, J. B., Smith, M., Pereira, L. S., Raes, D., Perrier, A., Alves, I., Walter, I., & Elliot, R. (2006). A recommendation on standardized surface resistance for hourly calculation of reference ET<sub>0</sub> by the FAO 56 Penman-Monteith method. *Agric. Water Mgmt.*, *81*(1-2), 1-22. <http://dx.doi.org/10.1016/j.agwat.2005.03.007>.
- Anderson, M. C., Norman, J. M., Kustas, W. P., Li, F., Prueger, J. H., & Mecikalski, J. R. (2005). Effects of vegetation clumping on two-source model estimates of surface energy fluxes from an agricultural landscape during SMACEX. *J. Hydrometeorol.*, *6*(6), 892-909. <http://dx.doi.org/10.1175/JHM465.1>.
- Anderson, M. C., Kustas, W. P., Alfieri, J. G., Gao, F., Hain, C., Prueger, J. H., Evett, S. R., Colaizzi, P., Howell, T. A., & Chavez, J. L. (2012). Mapping daily evapotranspiration at Landsat spatial scales during the BEAREX08 field campaign. *Adv. Water Resour.*, *50*, 162-177. <http://dx.doi.org/10.1016/j.advwatres.2012.06.005>.
- Baker, J. M., & van Bavel, C. H. M. (1987). Measurement of the mass flow of water in the stems of herbaceous plants. *Plant Cell Environ.*, *10*(9), 777-782.
- Brutsaert, W. (1982). *Evaporation into the Atmosphere: Theory, History, and Applications*. Dordrecht, The Netherlands: Kluwer. <http://dx.doi.org/10.1007/978-94-017-1497-6>.
- Campbell, G. S., & Norman, J. M. (1998). *An Introduction to Environmental Biophysics* (2nd ed.). New York, N.Y.: Springer-Verlag. <http://dx.doi.org/10.1007/978-1-4612-1626-1>.
- Chen, J. M., & Cihlar, J. (1995). Quantifying the effect of canopy architecture on optical measurements of leaf area index using two gap size analysis methods. *IEEE Trans. Geosci. Remote Sens.*, *33*(3), 777-787. <http://dx.doi.org/10.1109/36.387593>.
- Colaizzi, P. D., O'Shaughnessy, S. A., Gowda, P. H., Evett, S. R., Howell, T. A., Kustas, W. P., & Anderson, M. C. (2010). Radiometer footprint model to estimate sunlit and shaded components for row crops. *Agron. J.*, *102*(3), 942-955. <http://dx.doi.org/10.2134/agronj2009.0393>.
- Colaizzi, P. D., Evett, S. R., Howell, T. A., Gowda, P. H., O'Shaughnessy, S. A., Tolk, J. A., Kustas, W. P., & Anderson, M. C. (2012a). Two-source energy balance model: Rrefinements and lysimeter tests in the Southern High Plains. *Trans. ASABE*, *55*(2), 551-562. <http://dx.doi.org/10.13031/2013.41385>.
- Colaizzi, P. D., Evett, S. R., Howell, T. A., Li, F., Kustas, W. P., & Anderson, M. C. (2012b). Radiation model for row crops: I. Geometric model description and parameter optimization. *Agron. J.*, *104*(2), 225-240. <http://dx.doi.org/10.2134/agronj2011.0082>.
- Colaizzi, P. D., Schwartz, R. C., Evett, S. R., Howell, T. A., Gowda, P. H., & Tolk, J. A. (2012c). Radiation model for row crops: II. Model evaluation. *Agron. J.*, *104*(2), 241-255. <http://dx.doi.org/10.2134/agronj2011.0083>.
- Colaizzi, P. D., Kustas, W. P., Anderson, M. C., Agam, N., Tolk, J. A., Evett, S. R., Howell, T. A., Gowda, P. H., & O'Shaughnessy, S. A. (2012d). Two-source energy balance model estimates of evapotranspiration using component and composite surface temperatures. *Adv. Water Resour.*, *50*, 134-151. <http://dx.doi.org/10.1016/j.advwatres.2012.06.004>.
- Colaizzi, P. D., Agam, N., Tolk, J. A., Evett, S. R., Howell, T. A., Gowda, P. H., O'Shaughnessy, S. A., Kustas, W. P., & Anderson, M. C. (2014). Two-source energy balance model to calculate E, T, and ET: Comparison of Priestley-Taylor and Penman-Monteith formulations and two time scaling methods. *Trans. ASABE*, *57*(2), 479-498. <http://dx.doi.org/10.13031/trans.57.10423>.
- Colaizzi, P. D., Evett, S. R., Agam, N., Schwartz, R. C., & Kustas, W. P. (2016a). Soil heat flux calculation for sunlit and shaded surfaces under row crops: 1. Model development and sensitivity analysis. *Agric. Forest Meteorol.*, *216*, 115-128. <http://dx.doi.org/10.1016/j.agrformet.2015.10.010>.
- Colaizzi, P. D., Evett, S. R., Agam, N., Schwartz, R. C., Kustas, W.

- P., Cosh, M. H., & McKee, L. (2016b). Soil heat flux calculation for sunlit and shaded surfaces under row crops: 2. Model test. *Agric. Forest Meteorol.*, 216, 129-140. <http://dx.doi.org/10.1016/j.agrformet.2015.10.009>.
- Doorenbos, J., & Kassam, A. H. (1979). Yield response to water. Irrigation and Drainage Paper No. 33. Rome, Italy: United Nations FAO.
- Evet, S. R. (2000a). The TACQ program for automatic time domain reflectometry measurements: I. Design and operating characteristics. *Trans. ASAE*, 43(6), 1939-1946. <http://dx.doi.org/10.13031/2013.3099>.
- Evet, S. R. (2000b). The TACQ program for automatic time domain reflectometry measurements: II. Waveform interpretation methods. *Trans. ASAE*, 43(6), 1947-1956. <http://dx.doi.org/10.13031/2013.3100>.
- Evet, S. R., & Tolk, J. A. (2009). Introduction: Can water use efficiency be modeled well enough to impact crop management? *Agron. J.*, 101(3), 423-425. <http://dx.doi.org/10.2134/agronj2009.0038xs>.
- Evet, S. R., Warrick, A., & Matthias, A. (1995). Wall material and capping effects on microlysimeter temperatures and evaporation. *SSSA J.*, 59(2), 329-336. <http://dx.doi.org/10.2136/sssaj1995.03615995005900020009x>.
- Evet, S. R., Tolk, J. A., & Howell, T. A. (2005). Time domain reflectometry laboratory calibration in travel time, bulk electrical conductivity, and effective frequency. *Vadose Zone J.*, 4(4), 1020-1029. <http://dx.doi.org/10.2136/vzj2005.0046>.
- Evet, S. R., Kustas, W. P., Gowda, P. H., Anderson, M. C., Prueger, J. H., & Howell, T. A. (2012a). Overview of the Bushland evapotranspiration and agricultural remote sensing experiment 2008 (BEAREX08): A field experiment evaluating methods for quantifying ET at multiple scales. *Adv. Water Resour.*, 50, 4-19. <http://dx.doi.org/10.1016/j.advwatres.2012.03.010>.
- Evet, S. R., Schwartz, R. C., Howell, T. A., Baumhardt, R. L., & Copeland, K. S. (2012b). Can weighing lysimeter ET represent surrounding field ET well enough to test flux station measurements of daily and sub-daily ET? *Adv. Water Resour.*, 50, 79-90. <http://dx.doi.org/10.1016/j.advwatres.2012.07.023>.
- Evet, S. R., Agam, N., Kustas, W. P., Colaizzi, P. D., & Schwartz, R. C. (2012c). Soil profile method for soil thermal diffusivity, conductivity, and heat flux: Comparison to soil heat flux plates. *Adv. Water Resour.*, 50, 41-54. <http://dx.doi.org/10.1016/j.advwatres.2012.04.012>.
- Fitzgerald, G. J., Pinter Jr., P. J., Hunsaker, D. J., & Clarke, T. R. (2005). Multiple shadow fractions in spectral mixture analysis of a cotton canopy. *Remote Sens. Environ.*, 97(4), 526-539. <http://dx.doi.org/10.1016/j.rse.2005.05.020>.
- French, A. N., Hunsaker, D. J., Clarke, T. R., Fitzgerald, G. J., Lockett, W. E., & Pinter Jr., P. J. (2007). Energy balance estimation of evapotranspiration for wheat grown under variable management practices in central Arizona. *Trans. ASABE*, 50(6), 2059-2071. <http://dx.doi.org/10.13031/2013.24108>.
- French, A. N., Hunsaker, D. J., & Thorp, K. R. (2015). Remote sensing of evapotranspiration over cotton using the TSEB and METRIC energy balance models. *Remote Sens. Environ.*, 158, 281-294. <http://dx.doi.org/10.1016/j.rse.2014.11.003>.
- Gowda, P. H., Chávez, J. L., Colaizzi, P. D., Evett, S. R., Howell, T. A., & Tolk, J. A. (2008). ET mapping for agricultural water management: Present status and challenges. *Irrig. Sci.*, 26(3), 223-237. <http://dx.doi.org/10.1007/s00271-007-0088-6>.
- Howell, T. A. (1990). Wind profile parameter estimation using MathCAD. *Agron. J.*, 82(5), 1027-1030. <http://dx.doi.org/10.2134/agronj1990.00021962008200050038x>.
- Howell, T. A., Schneider, A. D., Dusek, D. A., Marek, T. H., & Steiner, J. L. (1995). Calibration and scale performance of Bushland weighing lysimeters. *Trans. ASAE*, 38(4), 1019-1024. <http://dx.doi.org/10.13031/2013.27918>.
- Howell, T. A., Steiner, J. L., Schneider, A. D., Evett, S. R., & Tolk, J. A. (1997). Seasonal and maximum daily evapotranspiration of irrigated winter wheat, sorghum, and corn: Southern High Plains. *Trans. ASAE*, 40(3), 623-634. <http://dx.doi.org/10.13031/2013.21321>.
- Howell, T. A., Evett, S. R., Schneider, A. D., Dusek, D. A., & Copeland, K. S. (2000). Irrigated fescue grass ET compared with calculated reference grass ET. In *Proc. 4th Dec. Natl. Irrig. Symp.* (pp. 228-242). St. Joseph, Mich.: ASAE.
- Idso, S. B. (1981). A set of equations for full spectrum and 8 to 14  $\mu\text{m}$  and 10.5 to 12.5  $\mu\text{m}$  thermal radiation from cloudless skies. *Water Resour. Res.*, 17(2), 295-304. <http://dx.doi.org/10.1029/WR017i002p00295>.
- Idso, S. B. (1983). Stomatal regulation of evaporation from well-watered plant canopies: A new synthesis. *Agric. Meteorol.*, 29(3), 213-217. [http://dx.doi.org/10.1016/0002-1571\(83\)90068-7](http://dx.doi.org/10.1016/0002-1571(83)90068-7).
- Idso, S. B., Jackson, R. D., Ehler, W. L., & Mitchell, S. T. (1969). A method for determination of infrared emittance of leaves. *Ecology*, 50(5), 899-902. <http://dx.doi.org/10.2307/1933705>.
- Idso, S. B., Reginato, R. J., Jackson, R. D., Kimball, B. A., & Nakayama, F. S. (1974). The three stages of drying of a field soil. *SSSA J.*, 38(5), 831-837. <http://dx.doi.org/10.2136/sssaj1974.03615995003800050037x>.
- Jackson, R. D. (1984). Remote sensing of vegetation characteristics for farm management. *Proc. SPIE*, 475, 81-96. <http://dx.doi.org/10.1117/12.966243>.
- Jackson, R. D., Idso, S. B., Reginato, R. J., & Pinter, P. J. (1981). Canopy temperature as a crop water stress indicator. *Water Resour. Res.*, 17(4), 1133-1138. <http://dx.doi.org/10.1029/WR017i004p01133>.
- Kimball, B. A., White, J. W., Ottman, M. J., Wall, G. W., Bernacchi, C. J., Morgan, J., & Smith, D. P. (2015). Predicting canopy temperatures and infrared heater energy requirements for warming field plots. *Agron. J.*, 107(1), 129-141. <http://dx.doi.org/10.2134/agronj14.0109>.
- Kimes, D. S. (1983). Remote sensing of row crop structure and component temperatures using directional radiometric temperatures and inversion techniques. *Remote Sens. Environ.*, 13(1), 33-55. [http://dx.doi.org/10.1016/0034-4257\(83\)90026-3](http://dx.doi.org/10.1016/0034-4257(83)90026-3).
- Kool, D., Agam, N., Lazarovitch, N., Heitman, J. L., Sauer, T. J., & Ben-Gal, A. (2014a). A review of approaches for evapotranspiration partitioning. *Agric. Forest Meteorol.*, 184, 56-70. <http://dx.doi.org/10.1016/j.agrformet.2013.09.003>.
- Kool, D., Ben-Gal, A., Agam, N., Šimůnek, J., Heitman, J. L., Sauer, T. J., & Lazarovitch, N. (2014b). Spatial and diurnal below canopy evaporation in a desert vineyard: Measurements and modeling. *Water Resour. Res.*, 50(8), 7035-7049. <http://dx.doi.org/10.1002/2014WR015409>.
- Kustas, W. P., & Anderson, M. C. (2009). Advances in thermal infrared remote sensing for land surface modeling. *Agric. Forest Meteorol.*, 149(12), 2071-2081. <http://dx.doi.org/10.1016/j.agrformet.2009.05.016>.
- Kustas, W. P., & Norman, J. M. (1999). Evaluation of soil and vegetation heat flux predictions using a simple two-source model with radiometric temperatures for partial canopy cover. *Agric. Forest Meteorol.*, 94(1), 13-29. [http://dx.doi.org/10.1016/S0168-1923\(99\)00005-2](http://dx.doi.org/10.1016/S0168-1923(99)00005-2).
- Kustas, W. P., Zhan, X., & Schmugge, T. J. (1998). Combining optical and microwave remote sensing for mapping energy fluxes in a semiarid watershed. *Remote Sens. Environ.*, 64(2), 116-131. [http://dx.doi.org/10.1016/S0034-4257\(97\)00176-4](http://dx.doi.org/10.1016/S0034-4257(97)00176-4).
- Kustas, W. P., Norman, J. M., Schmugge, T. J., & Anderson, M. C. (2004). Chapter 7: Mapping surface energy fluxes with

- radiometric temperature. In *Thermal Remote Sensing in Land Surface Processes* (pp. 205-254). Boca Raton, Fla.: CRC Press. <http://dx.doi.org/10.1201/9780203502174-c8>.
- Kustas, W. P., Alfieri, J. G., Anderson, M. C., Colaizzi, P. D., Prueger, J. H., Evett, S. R., Neal, C. M. U., French, A. N., Hipps, L. E., Chavez, J. L., Copeland, K. S., & Howell, T. A. (2012a). Evaluating the two-source energy balance model using local thermal and surface flux observations in a strongly advective irrigated agricultural area. *Adv. Water Resour.*, *50*, 120-133. <http://dx.doi.org/10.1016/j.advwatres.2012.07.005>.
- Kustas, W. P., Moran, M. S., & Meyers, T. P. (2012b). The Bushland evapotranspiration and agricultural remote sensing experiment 2008 (BEAREX08) special Issue. *Adv. Water Resour.*, *50*, 1-3. <http://dx.doi.org/10.1016/j.advwatres.2012.11.006>.
- Lascano, R. J., & van Bavel, C. H. M. (2007). Explicit and recursive calculation of potential and actual evapotranspiration. *Agron. J.*, *99*(2), 585-590. <http://dx.doi.org/10.2134/agronj2006.0159>.
- Lascano, R. J., van Bavel, C. H. M., & Evett, S. R. (2010). A field test of recursive calculation of crop evapotranspiration. *Trans. ASABE*, *53*(4), 1117-1126. <http://dx.doi.org/10.13031/2013.32601>.
- Legates, D. R., & McCabe Jr., G. J. (1999). Evaluating the use of "goodness-of-fit" measures in hydrologic and hydroclimatic model validation. *Water Resour. Res.*, *35*(1), 233-241. <http://dx.doi.org/10.1029/1998WR900018>.
- Li, F., Kustas, W. P., Prueger, J. H., Neal, C. M., & Jackson, T. J. (2005). Utility of remote sensing-based two-source energy balance model under low- and high-vegetation cover conditions. *J. Hydrometeorol.*, *6*(6), 878-891. <http://dx.doi.org/10.1175/JHM464.1>.
- Mahrt, L., & Ek, M. (1984). The influence of atmospheric stability on potential evapotranspiration. *J. Clim. Appl. Meteorol.*, *23*(2), 222-234. [http://dx.doi.org/10.1175/1520-0450\(1984\)023%3C0222%3ATIOASO%3E2.0.CO%3B2](http://dx.doi.org/10.1175/1520-0450(1984)023%3C0222%3ATIOASO%3E2.0.CO%3B2).
- Marek, G. W., Evett, S. R., Gowda, P. H., Howell, T. A., Copeland, K. S., & Baumhardt, R. L. (2014). Post-processing techniques for reducing errors in weighing lysimeter evapotranspiration (ET) datasets. *Trans. ASABE*, *57*(2), 499-515. <http://dx.doi.org/10.13031/trans.57.10433>.
- Marek, T. H., Schneider, A. D., Howell, T. A., & Ebeling, L. L. (1988). Design and construction of large weighing monolithic lysimeters. *Trans. ASAE*, *31*(2), 477-484. <http://dx.doi.org/10.13031/2013.30734>.
- Monteith, J. L. (1973). *Principles of Environmental Physics*. London, U.K.: Edward Arnold.
- Nash, J. E., & Sutcliffe, J. V. (1970). River flow forecasting through conceptual models: Part 1. A discussion of principles. *J. Hydrol.*, *10*(3), 282-290. [http://dx.doi.org/10.1016/0022-1694\(70\)90255-6](http://dx.doi.org/10.1016/0022-1694(70)90255-6).
- Newman, B. D., Wilcox, B. P., Archer, S. R., Breshears, D. D., Dahm, C. N., Duffy, C. J., McDowell, N. G., Phillips, F. M., Scanlon, B. R., & Vivoni, E. R. (2006). Ecohydrology of water-limited environments: A scientific vision. *Water Resour. Res.*, *42*(6), W06302. <http://dx.doi.org/10.1029/2005WR004141>.
- Norman, J. M., & Becker, F. (1995). Terminology in thermal infrared remote sensing of natural surfaces. *Remote Sensing Rev.*, *12*(3-4), 159-173. <http://dx.doi.org/10.1080/02757259509532284>.
- Norman, J. M., Kustas, W. P., & Humes, K. S. (1995). Source approach for estimating soil and vegetation energy fluxes in observations of directional radiometric surface temperature. *Agric. Forest Meteorol.*, *77*(3-4), 263-293. [http://dx.doi.org/10.1016/0168-1923\(95\)02265-Y](http://dx.doi.org/10.1016/0168-1923(95)02265-Y).
- Norman, J. M., Kustas, W. P., Prueger, J. H., & Diak, G. H. (2000). Surface flux estimation using radiometric temperature: A dual temperature difference method to minimize measurement errors. *Water Resour. Res.*, *36*(8), 2263-2274. <http://dx.doi.org/10.1029/2000WR900033>.
- Novak, M. D. (2010). Dynamics of the near-surface evaporation zone and corresponding effects on the surface energy balance of a drying bare soil. *Agric. Forest Meteorol.*, *150*(10), 1358-1365. <http://dx.doi.org/10.1016/j.agrformet.2010.06.005>.
- O'Shaughnessy, S. A., & Evett, S. R. (2010). Canopy temperature based system effectively schedules and controls center-pivot irrigation of cotton. *Agric. Water Mgmt.*, *97*(9), 1310-1316. <http://dx.doi.org/10.1016/j.agwat.2010.03.012>.
- O'Shaughnessy, S. A., Evett, S. R., Colaizzi, P. D., & Howell, T. A. (2011). Using radiation thermography and thermometry to evaluate crop water stress in soybean and cotton. *Agric. Water Mgmt.*, *98*(10), 1523-1535. <http://dx.doi.org/10.1016/j.agwat.2011.05.005>.
- O'Shaughnessy, S. A., Evett, S. R., Colaizzi, P. D., & Howell, T. A. (2012). A crop water stress index and time threshold for automatic irrigation scheduling of grain sorghum. *Agric. Water Mgmt.*, *107*, 122-132. <http://dx.doi.org/10.1016/j.agwat.2012.01.018>.
- O'Shaughnessy, S. A., Evett, S. R., Colaizzi, P. D., & Howell, T. A. (2013). Wireless sensor network effectively controls center-pivot irrigation of sorghum. *Appl. Eng. Agric.*, *29*(6), 853-864. <http://dx.doi.org/10.13031/aea.29.9921>.
- Peters, R. T., & Evett, S. R. (2008). Automation of a center pivot using the temperature-time-threshold method of irrigation scheduling. *J. Irrig. Drain.*, *134*(3), 286-291. [http://dx.doi.org/10.1061/\(ASCE\)0733-9437\(2008\)134:3\(286\)](http://dx.doi.org/10.1061/(ASCE)0733-9437(2008)134:3(286)).
- Priestley, R., & Taylor, R. (1972). On the assessment of surface heat flux and evaporation using large-scale parameters. *Monthly Weather Rev.*, *100*(2), 81-92. [http://dx.doi.org/10.1175/1520-0493\(1972\)100<0081:OTAOSH>2.3.CO;2](http://dx.doi.org/10.1175/1520-0493(1972)100<0081:OTAOSH>2.3.CO;2).
- Santanello Jr., J. A., & Friedl, M. A. (2003). Diurnal covariation in soil heat flux and net radiation. *J. Appl. Meteorol.*, *42*(6), 851-862. [http://dx.doi.org/10.1175/1520-0450\(2003\)042<0851:DCISHF>2.0.CO;2](http://dx.doi.org/10.1175/1520-0450(2003)042<0851:DCISHF>2.0.CO;2).
- Schlesinger, W. H., & Jasechko, S. (2014). Transpiration in the global water cycle. *Agric. Forest Meteorol.*, *189-190*, 115-117. <http://dx.doi.org/10.1016/j.agrformet.2014.01.011>.
- Schneider, A. D., & Howell, T. A. (2000). Surface runoff due to LEPA and spray irrigation of a slowly permeable soil. *Trans. ASAE*, *43*(5), 1089-1095. <http://dx.doi.org/10.13031/2013.3001>.
- Sutanto, S. J., van den Hurk, B., Dirmeyer, P. A., Seneviratne, S. I., Röckmann, T., Trenberth, K. E., Blyth, E. M., Wenninger, J., & Hoffmann, G. (2014). A perspective on isotope versus non-isotope approaches to determine the contribution of transpiration to total evaporation. *Earth Syst. Sci.*, *118*(8), 2815-2827. <http://dx.doi.org/10.5194/hess-18-2815-2014>.
- Todd, R. W., Evett, S. R., & Howell, T. A. (2000). The Bowen ratio energy balance method for estimating latent heat flux of irrigated alfalfa evaluated in a semi-arid, advective environment. *Agric. Forest Meteorol.*, *103*(4), 335-348. [http://dx.doi.org/10.1016/S0168-1923\(00\)00139-8](http://dx.doi.org/10.1016/S0168-1923(00)00139-8).
- Tolk, J. A., Howell, T. A., & Evett, S. R. (2006a). Nighttime evapotranspiration from alfalfa and cotton in a semiarid climate. *Agron. J.*, *98*(3), 730-736. <http://dx.doi.org/10.2134/agronj2005.0276>.
- Tolk, J. A., Evett, S. R., & Howell, T. A. (2006b). Advection influences on evapotranspiration of alfalfa in a semiarid climate. *Agron. J.*, *98*(6), 1646-1654. <http://dx.doi.org/10.2134/agronj2006.0031>.
- Twine, T. E., Kustas, W. P., Norman, J. M., Cook, D. R., Houser, P. R., Meyers, T. P., Prueger, J. H., Starks, P. J., & Wesley, M. L. (2000). Correcting eddy-covariance flux underestimates over a grassland. *Agric. Forest Meteorol.*, *103*(3), 279-300.

[http://dx.doi.org/10.1016/S0168-1923\(00\)00123-4](http://dx.doi.org/10.1016/S0168-1923(00)00123-4).  
USDA-NRCS. (2015). Soil survey TX375: Potter County, Texas.  
Washington, D.C.: USDA Natural Resources Conservation  
Service. Retrieved from <http://websoilsurvey.nrcs.usda.gov>.  
Wanjura, D. F., & Upchurch, D. R. (1996). Time thresholds for  
canopy temperature-based irrigation. In *Proc. Intl. Conf.*

*Evapotranspiration Irrig. Scheduling* (pp. 295-303). St. Joseph,  
Mich.: ASAE.  
Wanjura, D. F., Maas, S. J., Winslow, J. C., & Upchurch, D. R.  
(2004). Scanned and spot-measured canopy temperatures of  
cotton and corn. *Comput. Electron. Agric.*, 44(1), 33-48.  
<http://dx.doi.org/10.1016/j.compag.2004.02.005>.